Fatigue and Dynamic Loading

Fatigue failure:

Often, machine members are found to have failed under the action of repeated or fluctuating stresses; yet the most careful analysis reveals that the actual maximum stresses were well below the ultimate strength of the material, and quite frequently even below the yield strength. The most distinguishing characteristic of these failures is that the stresses have been repeated a very large number of times. Hence the failure is called a *fatigue failure*.

When machine parts fail statically, they usually develop a very large deflection, because the stress has exceeded the yield strength, and the part is replaced before fracture actually occurs. Thus many static failures give visible warning in advance. But a fatigue failure gives no warning! It is sudden and total, and hence dangerous. It is relatively simple to design against a static failure, because our knowledge is comprehensive. Fatigue is a much more complicated phenomenon, only partially understood, and the engineer seeking competence must acquire as much knowledge of the subject as possible.

- Static conditions : loads are applied gradually, to give sufficient time for the strain to fully develop.
- Variable conditions : stresses vary with time or fluctuate between different levels, also called repeated, alternating, or fluctuating stresses.
- When machine members are found to have failed under fluctuating stresses, the actual maximum stresses were well below the ultimate strength of the material, even below yielding strength.
- Since these failures are due to stresses repeating for a large number of times, they are called fatigue failures.
- When machine parts fails statically, they usually develop a very large deflection, thus visible warning can be observed in advance; a fatigue failure gives no warning!

A fatigue failure has an appearance similar to a brittle fracture, as the fracture surfaces are flat and perpendicular to the stress axis with the absence of necking.

- A fatigue failure arises from three stages of development:
    - Stage I : initiation of microcracks due to cyclic plastic deformation (these cracks are not usually visible to the naked eyes).
    - Stage II : propagation of microcracks to macrocracks forming parallel plateau0like fracture surfaces separated by longitudinal ridges (in the form of dark and light bands referred to as beach marks).
    - Stage III : fracture when the remaining material cannot support the loads.

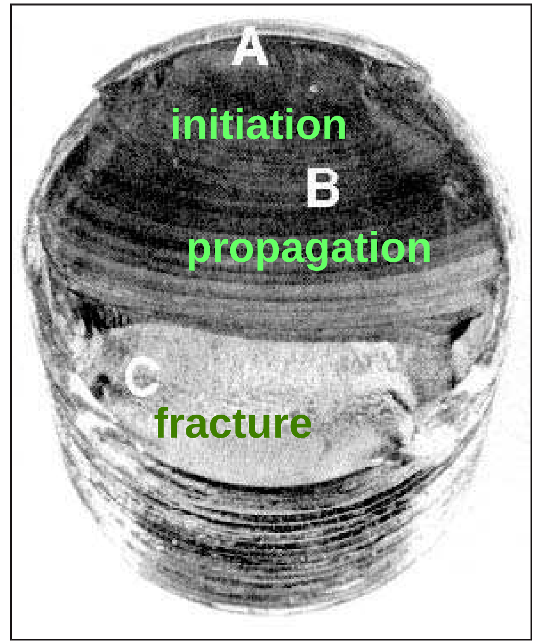

6–11 Characterizing Fluctuating Stresses

Fluctuating stresses in machinery often take the form of a sinusoidal pattern because of the nature of some rotating machinery. However, other patterns, some quite irregular, do occur. It has been found that in periodic patterns exhibiting a single maximum and a single minimum of force, the shape of the wave is not important, but the peaks on both the high side (maximum) and the low side (minimum) are important. Thus F_{max} and F_{min} in a cycle of force can be used to characterize the force pattern. It is also true that ranging above and below some baseline can be equally effective in characterizing the force pattern. If the largest force is F_{max} and the smallest force is F_{min}, then a steady component and an alternating component can be constructed as follows:

$$F_m = \frac{F_{max} + F_{min}}{2} \qquad F_a = \left| \frac{F_{max} - F_{min}}{2} \right|$$

where F_m is the midrange steady component of force, and F_a is the amplitude of the alternating component of force.

Figure 6–23

Some stress-time relations: (*a*) fluctuating stress with high-frequency ripple; (*b* and *c*) nonsinusoidal fluctuating stress; (*d*) sinusoidal fluctuating stress; (*e*) repeated stress; (*f*) completely reversed sinusoidal stress.

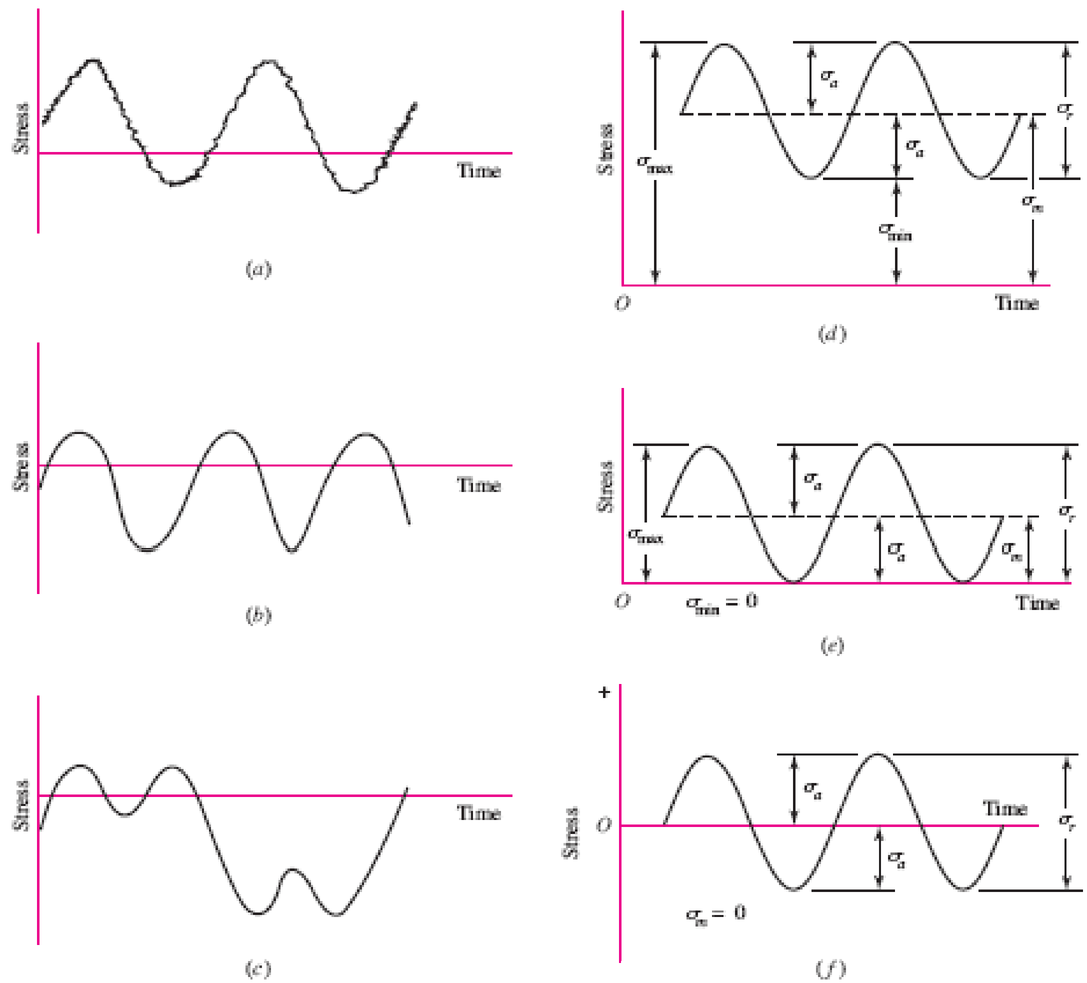

$$\sigma_m = \frac{\sigma_{\max} + \sigma_{\min}}{2}$$

$$\sigma_a = \left| \frac{\sigma_{\max} - \sigma_{\min}}{2} \right|$$

In addition to Eq. (6–36), the *stress ratio*

$$R = \frac{\sigma_{\min}}{\sigma_{\max}}$$

and the *amplitude ratio*

$$A = \frac{\sigma_a}{\sigma_m}$$

Figure 6–23 illustrates some of the various stress-time traces that occur. The components of stress, some of which are shown in Fig. 6–23*d*, are

σ_{min} = minimum stress

σ_{max} = maximum stress

σ_a = amplitude component

σ_m = midrange component

σ_r = range of stress

σ_s = static or steady stress

Fatigue Life Methods in Fatigue Failure Analysis

- Let N be the number of cycles to fatigue for a specified level of loading
  - For $1 \leq N \leq 10^3$, generally classified as low-cycle fatigue
  - For $N > 10^3$, generally classified as high-cycle fatigue
- Three major fatigue life methods used in design and analysis are
  - ü <u>stress-life method</u> : is based on stress only, least accurate especially for low-cycle fatigue; however, it is the most traditional and easiest to implement for a wide range of applications.
  - ü <u>strain-life method</u> : involves more detailed analysis, especially good for low-cycle fatigue; however, idealizations in the methods make it less practical when uncertainties are present.
  - ü <u>linear-elastic fracture mechanics method</u> : assumes a crack is already present. Practical with computer codes in predicting in crack growth with respect to stress intensity factor

6–2 Approach to Fatigue Failure in Analysis and Design

In this chapter, we will take a structured approach in the design against fatigue failure. As with static failure, we will attempt to relate to test results performed on simply loaded specimens. However, because of the complex nature of fatigue, there is much more to account for. From this point, we will proceed methodically, and in stages. In an attempt to provide some insight as to what follows in this chapter, a brief description of the remaining sections will be given here.

6–4 The Stress-Life Method

To determine the strength of materials under the action of fatigue loads, specimens are subjected to repeated or varying forces of specified magnitudes while the cycles or stress reversals are counted to destruction. The most widely used fatigue-testing device

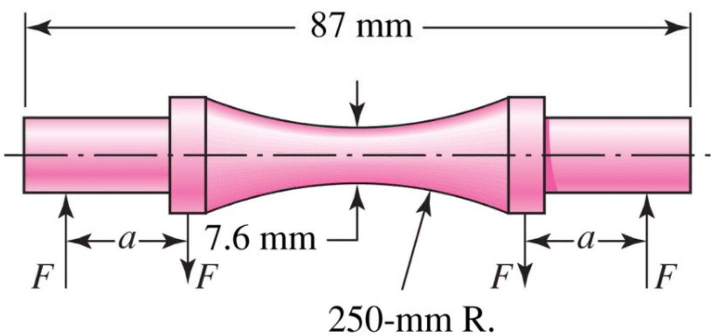

- The most widely used fatigue-testing device is the R. R. Moore high-speed rotating-beam machine.
- Specimens in R.R. Moore machines are subjected to pure bending by means of added weights.
- Other fatigue-testing machines are available for applying fluctuating or reversed axial stresses, torsional stresses, or combined stresses to the test specimens.

S-N Curve

- In R. R. Moore machine tests, a constant bending load is applied, and the number of revolutions of the beam required for failure is recorded.
- Tests at various bending stress levels are conducted.
- These results are plotted as an *S-N* diagram.
- Log plot is generally used to emphasize the bend in the S-N curve.
- Ordinate of S-N curve is fatigue strength, S_f , at a specific number of cycles

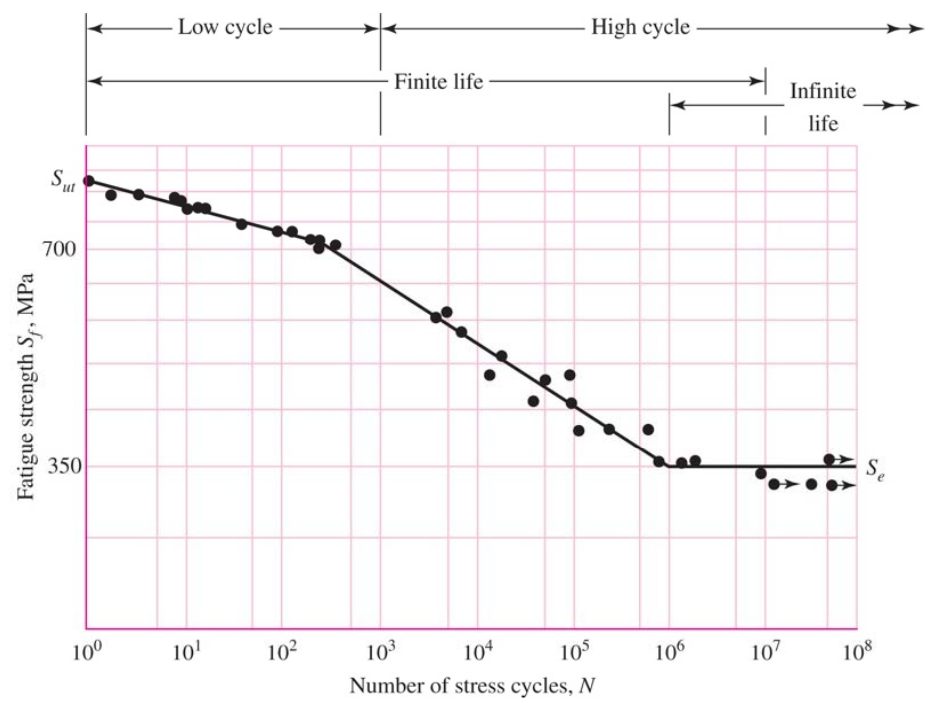

S-N diagram from the results of completely reversed axial fatigue test. Material : UNS G41300 steel.

Characteristics of S-N Curves for Metals

- In the case of steels, a knee occurs in the graph, and beyond this knee failure will not occur, no matter how great the number of cycles - this knee is called the *endurance limit*, denoted as S_e
- Non-ferrous metals and alloys do not have an endurance limit, since their S-N curve never become horizontal.
- For materials with no endurance limit, the fatigue strength is normally reported at $N = 5 \times 10^8$
- $N = 1/2$ is the simple tension test

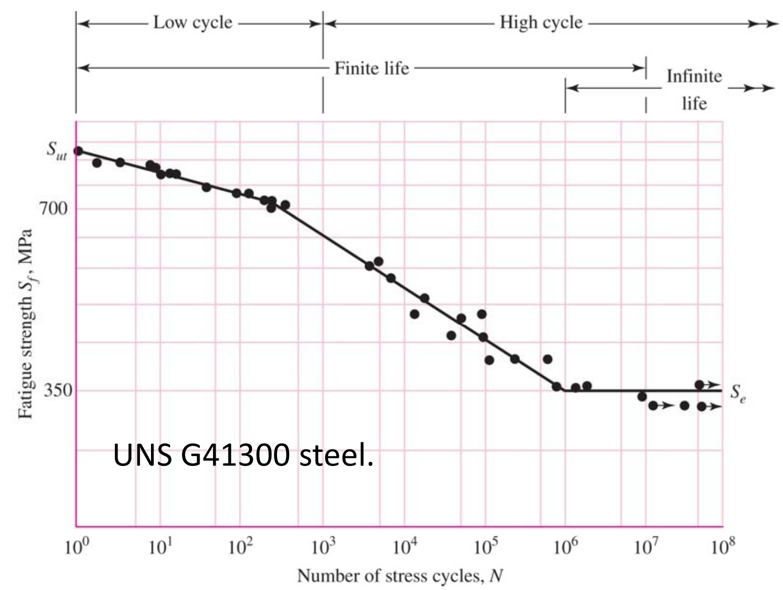

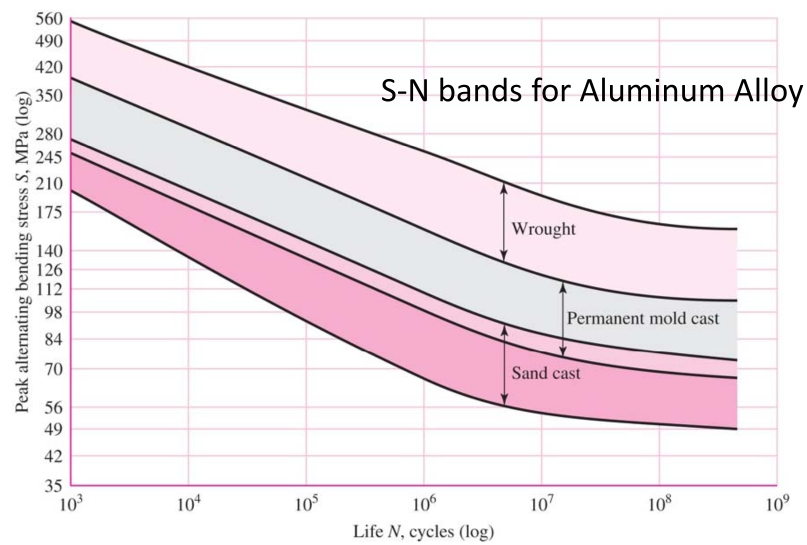

We note that a stress cycle ($N = 1$) constitutes a single application and removal of a load and then another application and removal of the load in the opposite direction. Thus $N = \frac{1}{2}$ means the load is applied once and then removed, which is the case with the simple tension test.

The body of knowledge available on fatigue failure from $N = 1$ to $N = 1000$ cycles is generally classified as *low-cycle fatigue*, as indicated in Fig. 6–10. *High-cycle fatigue*, then, is concerned with failure corresponding to stress cycles greater than 10^3 cycles.

We also distinguish a *finite-life region* and an *infinite-life region* in Fig. 6–10. The boundary between these regions cannot be clearly defined except for a specific material; but it lies somewhere between 10^6 and 10^7 cycles for steels, as shown in Fig. 6–10.

As stated earlier, the stress-life method is the least accurate approach especially for low-cycle applications. However, it is the most traditional method, with much published data available. It is the easiest to implement for a wide range of design applications and represents high-cycle applications adequately. For these reasons the stress-life method will be emphasized in subsequent sections of this chapter.

Table A–23

Mean Monotonic and Cyclic Stress-Strain Properties of Selected Steels *Source: ASM Metals Reference Book, 2nd ed., American Society for Metals, Metals Park, Ohio, 1983, p. 217.*

Grade (a)	Orientation (e)	Description (f)	Hardness HB	Tensile Strength S_{ut} MPa	Tensile Strength S_{ut} ksi	Reduction in Area %	True Strain at Fracture ε_f	Modulus of Elasticity E GPa	Modulus of Elasticity E 10^6 psi	Fatigue Strength Coefficient σ'_f MPa	Fatigue Strength Coefficient σ'_f ksi	Fatigue Strength Exponent b	Fatigue Ductility Coefficient ε'_F	Fatigue Ductility Exponent c
A538A (b)	L	STA	405	1515	220	67	1.10	185	27	1655	240	−0.065	0.30	−0.62
A538B (b)	L	STA	460	1860	270	56	0.82	185	27	2135	310	−0.071	0.80	−0.71
A538C (b)	L	STA	480	2000	290	55	0.81	180	26	2240	325	−0.07	0.60	−0.75
AM350 (c)	L	HR, A		1315	191	52	0.74	195	28	2800	406	−0.14	0.33	−0.84
AM350 (c)	L	CD	496	1905	276	20	0.23	180	26	2690	390	−0.102	0.10	−0.42
Gainex (c)	LT	HR sheet		530	77	58	0.86	200	29.2	805	117	−0.07	0.86	−0.65
Gainex (c)	L	HR sheet		510	74	64	1.02	200	29.2	805	117	−0.071	0.86	−0.68
H-11	L	Ausformed	660	2585	375	33	0.40	205	30	3170	460	−0.077	0.08	−0.74
RQC-100 (c)	LT	HR plate	290	940	136	43	0.56	205	30	1240	180	−0.07	0.66	−0.69
RQC-100 (c)	L	HR plate	290	930	135	67	1.02	205	30	1240	180	−0.07	0.66	−0.69
10B62	L	Q&T	430	1640	238	38	0.89	195	28	1780	258	−0.067	0.32	−0.56
1005-1009	LT	HR sheet	90	360	52	73	1.3	205	30	580	84	−0.09	0.15	−0.43
1005-1009	LT	CD sheet	125	470	68	66	1.09	205	30	515	75	−0.059	0.30	−0.51
1005-1009	L	CD sheet	125	415	60	64	1.02	200	29	540	78	−0.073	0.11	−0.41
1005-1009	L	HR sheet	90	345	50	80	1.6	200	29	640	93	−0.109	0.10	−0.39
1015	L	Normalized	80	415	60	68	1.14	205	30	825	120	−0.11	0.95	−0.64
1020	L	HR plate	108	440	64	62	0.96	205	29.5	895	130	−0.12	0.41	−0.51
1040	L	As forged	225	620	90	60	0.93	200	29	1540	223	−0.14	0.61	−0.57
1045	L	Q&T	225	725	105	65	1.04	200	29	1225	178	−0.095	1.00	−0.66
1045	L	Q&T	410	1450	210	51	0.72	200	29	1860	270	−0.073	0.60	−0.70
1045	L	Q&T	390	1345	195	59	0.89	205	30	1585	230	−0.074	0.45	−0.68
1045	L	Q&T	450	1585	230	55	0.81	205	30	1795	260	−0.07	0.35	−0.69
1045	L	Q&T	500	1825	265	51	0.71	205	30	2275	330	−0.08	0.25	−0.68
1045	L	Q&T	595	2240	325	41	0.52	205	30	2725	395	−0.081	0.07	−0.60
1144	L	CDSR	265	930	135	33	0.51	195	28.5	1000	145	−0.08	0.32	−0.58

6–7 The Endurance Limit

The determination of endurance limits by fatigue testing is now routine, though a lengthy procedure. Generally, stress testing is preferred to strain testing for endurance limits.

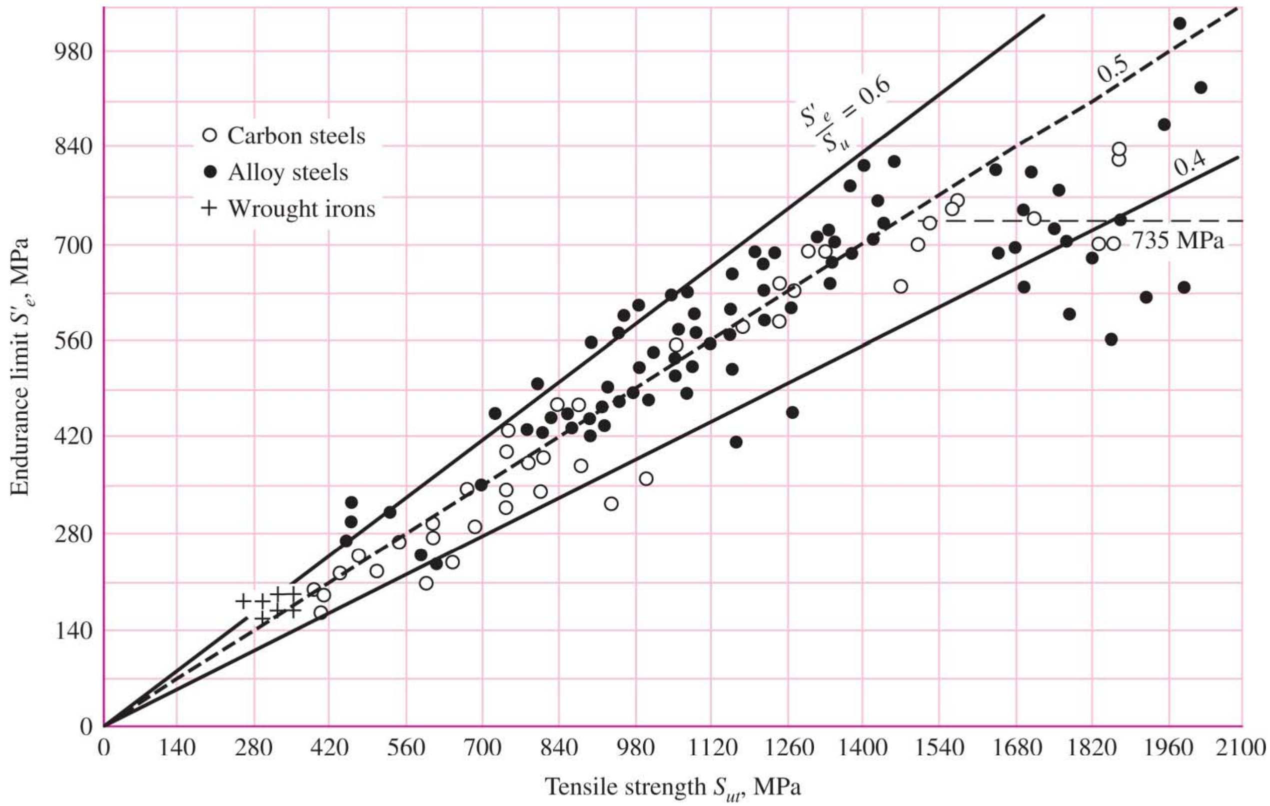

Figure 6–17

Graph of endurance limits versus tensile strengths from actual test results for a large number of wrought irons and steels. Ratios of S'_e/S_{ut} of 0.60, 0.50, and 0.40 are shown by the solid and dashed lines. Note also the horizontal dashed line for $S'_e = 735$ MPa. Points shown having a tensile strength greater than 1470 MPa have a mean endurance limit of $S'_e = 735$ MPa and a standard deviation of 95 MPa. *(Collated from data compiled by H. J. Grover, S. A. Gordon, and L. R. Jackson in* Fatigue of Metals and Structures, *Bureau of Naval Weapons Document NAVWEPS 00-25-534, 1960; and from* Fatigue Design Handbook, *SAE, 1968, p. 42.)*

$$S'_e = \begin{cases} 0.5S_{ut}, & S_{ut} \leq 1400\text{MPa} \\ 700\text{MPa}, & S_{ut} > 1400\text{MPa} \end{cases}$$

Steels treated to give different microstructures have different S'_e/S_{ut} ratios. It appears that the more ductile microstructures have a higher ratio. Martensite has a very brittle nature and is highly susceptible to fatigue-induced cracking; thus the ratio is low. When designs include detailed heat-treating specifications to obtain specific microstructures, it is possible to use an estimate of the endurance limit based on test data for the particular microstructure; such estimates are much more reliable and indeed should be used.

The endurance limits for various classes of cast irons, polished or machined, are given in Table A–24. Aluminum alloys do not have an endurance limit. The fatigue strengths of some aluminum alloys at $5(10^8)$ cycles of reversed stress are given in Table A–24.

Table A–24

Mechanical Properties of Three Non-Steel Metals

(a) Typical Properties of Gray Cast Iron

[The American Society for Testing and Materials (ASTM) numbering system for gray cast iron is such that the numbers correspond to the *minimum tensile strength* in kpsi. Thus an ASTM No. 20 cast iron has a minimum tensile strength of 138 MPa (20 kpsi). Note particularly that the tabulations are *typical* of several heats.]

ASTM Number	Tensile Strength S_{ut}, MPa (kpsi)	Compressive Strength S_{uc}, MPa (kpsi)	Shear Modulus of Rupture S_{su}, MPa (kpsi)	Modulus of Elasticity, Mpsi: Tension†	Modulus of Elasticity, Mpsi: Torsion	Endurance Limit* S_e, MPa (kpsi)	Brinell Hardness H_B	Fatigue Stress-Concentration Factor K_f
20	152 (22)	572 (83)	179 (26)	9.6–14	3.9–5.6	69 (10)	156	1.00
25	179 (26)	669 (97)	220 (32)	11.5–14.8	4.6–6.0	79 (11.5)	174	1.05
30	214 (31)	752 (109)	276 (40)	13–16.4	5.2–6.6	97 (14)	201	1.10
35	252 (36.5)	855 (124)	334 (48.5)	14.5–17.2	5.8–6.9	110 (16)	212	1.15
40	293 (42.5)	970 (140)	393 (57)	16–20	6.4–7.8	128 (18.5)	235	1.25
50	362 (52.5)	1130 (164)	503 (73)	18.8–22.8	7.2–8.0	148 (21.5)	262	1.35
60	431 (62.5)	1293 (187.5)	610 (88.5)	20.4–23.5	7.8–8.5	169 (24.5)	302	1.50

*Polished or machined specimens.

†The modulus of elasticity of cast iron in compression corresponds closely to the upper value in the range given for tension and is a more constant value than that for tension.

Table A–24

Mechanical Properties of Three Non-Steel Metals *(Continued)*

(b) Mechanical Properties of Some Aluminum Alloys

[These *are typical* properties for sizes of about $\frac{1}{2}$ in; similar properties can be obtained by using proper purcha

specifications. The values given for fatigue strength correspond to $50(10^7)$ cycles of completely reversed stress

Alluminum alloys do not have an endurance limit. Yield strengths were obtained by the 0.2 percent offset metl

Aluminum Association Number	Temper	Yield, S_y, MPa (kpsi)	Strength Tensile, S_u, MPa (kpsi)	Fatigue, S_f, MPa (kpsi)	Elongation in 2 in, %	Brinell Hardness H_B
Wrought:						
2017	O	70 (10)	179 (26)	90 (13)	22	45
2024	O	76 (11)	186 (27)	90 (13)	22	47
	T3	345 (50)	482 (70)	138 (20)	16	120
3003	H12	117 (17)	131 (19)	55 (8)	20	35
	H16	165 (24)	179 (26)	65 (9.5)	14	47
3004	H34	186 (27)	234 (34)	103 (15)	12	63
	H38	234 (34)	276 (40)	110 (16)	6	77
5052	H32	186 (27)	234 (34)	117 (17)	18	62
	H36	234 (34)	269 (39)	124 (18)	10	74
Cast:						
319.0*	T6	165 (24)	248 (36)	69 (10)	2.0	80
333.0†	T5	172 (25)	234 (34)	83 (12)	1.0	100
	T6	207 (30)	289 (42)	103 (15)	1.5	105
335.0*	T6	172 (25)	241 (35)	62 (9)	3.0	80
	T7	248 (36)	262 (38)	62 (9)	0.5	85

*Sand casting.

†Permanent-mold casting.

(c) Mechanical Properties of Some Titanium Alloys

Titanium Alloy	Condition	Yield, S_y (0.2% offset) MPa (kpsi)	Strength Tensile, S_{ut} MPa (kpsi)	Elongation in 2 in, %	Hardness (Brinell or Rockwell)
Ti-35A†	Annealed	210 (30)	275 (40)	30	135 HB
Ti-50A†	Annealed	310 (45)	380 (55)	25	215 HB
Ti-0.2 Pd	Annealed	280 (40)	340 (50)	28	200 HB
Ti-5 Al-2.5 Sn	Annealed	760 (110)	790 (115)	16	36 HRC
Ti-8 Al-1 Mo-1 V	Annealed	900 (130)	965 (140)	15	39 HRC
Ti-6 Al-6 V-2 Sn	Annealed	970 (140)	1030 (150)	14	38 HRC
Ti-6Al-4V	Annealed	830 (120)	900 (130)	14	36 HRC
Ti-13 V-11 Cr-3 Al	Sol. + aging	1207 (175)	1276 (185)	8	40 HRC

†Commercially pure alpha titanium.

Fatigue Strength : Basics

- Low-cycle fatigue considers the range from N=1 to about 1000 cycles.
- In this region, the fatigue strength S_f is only slightly smaller than the tensile strength S_{ut} .
- High-cycle fatigue domain extends from 10^3 to the endurance limit life (10^6 to 10^7 cycles).
- Experience has shown that high-cycle fatigue data are rectified by a logarithmic transform to both stress and cycles-to-failure.

Fatigue Strength at Different *N*

- Define the fatigue strength at a specified number of cycles as $(S'_f)_N$
- By combining the elastic strain relations, we can get

$$(S'_f)_N \doteq E\,\Delta\varepsilon_e/2, \qquad (S'_f)_N = \sigma'_F(2N)^b$$

- Define f as the fraction of tensile strength to $(S'_f)_{10^3}$. The value of f at 10^3 cycles is then

$$f = \frac{\sigma'_F}{S_{ut}}(2 \cdot 10^3)^b$$

- To find b, substitute the endurance strength (S'_e)and the corresponding cycles (N_e) and solving for b as

$$b = -\frac{\log(\sigma'_F/S'_e)}{\log(2N_e)}$$

- For example, for steels when

$$\sigma'_F = S_{ut} + 345 \qquad S'_e = 366\text{MPa}$$
$$S_{ut} = 735\text{MPa} \qquad N_e = 10^6$$
$$\Rightarrow \quad S'_f = 1030N^{-0.0749}$$

Fatigue Strength and estimates of fatigue life

Figure 6–18

Fatigue strength fraction, f, of S_{ut} at 10^3 cycles for $S_e = S'_e = 0.5S_{ut}$ at 10^6 cycles.

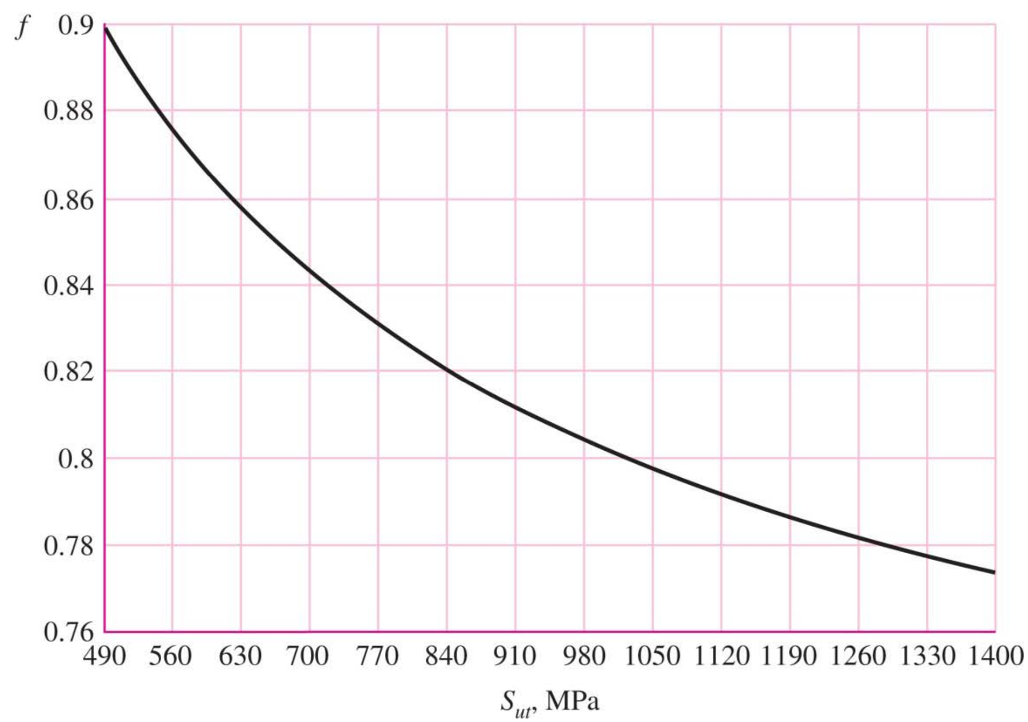

490 MPa < S_{ut} <1400 MPa (use the plot) , S_{ut}< 350 MPa, f=0.9

$$S_f = a\,N^b \tag{6–13}$$

where N is cycles to failure and the constants a and b are defined by the points $10^3, (S_f)_{10^3}$ and $10^6, S_e$ with $(S_f)_{10^3} = f\,S_{ut}$. Substituting these two points in Eq. (6–13) gives

$$a = \frac{(f\,S_{ut})^2}{S_e} \tag{6–14}$$

$$b = -\frac{1}{3}\log\left(\frac{f\,S_{ut}}{S_e}\right) \tag{6–15}$$

$$N = \left(\frac{\sigma_a}{a}\right)^{1/b}$$

EXAMPLE 6–2 Given a 1050 HR steel, *estimate*

(*a*) the rotating-beam endurance limit at 10^6 cycles.

(*b*) the endurance strength of a polished rotating-beam specimen corresponding to 10^4 cycles to failure

(*c*) the expected life of a polished rotating-beam specimen under a completely reversed stress of 385 MPa.

Solution (*a*) From Table A–20, $S_{ut} = 630$ MPa. From Eq. (6–8),

Answer

$$S'_e = 0.5(630) = 315 \text{ MPa}$$

(*b*) From Fig. 6–18, for $S_{ut} = 630$ MPa, $f \doteq 0.86$. From Eq. (6–14),

$$a = \frac{[0.86(630)^2]}{315} = 1084 \text{ MPa}$$

From Eq. (6–15),

$$b = -\frac{1}{3}\log\left[\frac{0.86(630)}{315}\right] = -0.0785$$

Thus, Eq. (6–13) is

$$S'_f = 1084\, N^{-0.0785}$$

Answer For 10^4 cycles to failure, $S'_f = 1084(10^4)^{-0.0785} = 526$ MPa

(*c*) From Eq. (6–16), with $\sigma_a = 385$ MPa,

Answer

$$N = \left(\frac{385}{1084}\right)^{1/-0.0785} = 53.3(10^4)\text{cycles}$$

Keep in mind that these are only *estimates.* So expressing the answers using three-place accuracy is a little misleading.

6–9 Endurance Limit Modifying Factors

We have seen that the rotating-beam specimen used in the laboratory to determine endurance limits is prepared very carefully and tested under closely controlled conditions. It is unrealistic to expect the endurance limit of a mechanical or structural member to match the values obtained in the laboratory. Some differences include

- *Material:* composition, basis of failure, variability
- *Manufacturing:* method, heat treatment, fretting corrosion, surface condition, stress concentration
- *Environment:* corrosion, temperature, stress state, relaxation times
- *Design:* size, shape, life, stress state, stress concentration, speed, fretting, galling

$$S_e = k_a k_b k_c k_d k_e k_f S_e' \tag{6–18}$$

where
k_a = surface condition modification factor
k_b = size modification factor
k_c = load modification factor
k_d = temperature modification factor
k_e = reliability factor[13]
k_f = miscellaneous-effects modification factor
S_e' = rotary-beam test specimen endurance limit
S_e = endurance limit at the critical location of a machine part in the geometry and condition of use

Surface Factor k_a

The surface of a rotating-beam specimen is highly polished, with a final polishing in the axial direction to smooth out any circumferential scratches. The surface modification factor depends on the quality of the finish of the actual part surface and on the tensile strength of the part material. To find quantitative expressions for common finishes of machine parts (ground, machined, or cold-drawn, hot-rolled, and as-forged), the coordinates of data points were recaptured from a plot of endurance limit versus ultimate tensile strength of data gathered by Lipson and Noll and reproduced by Horger.[14] The data can be represented by

$$k_a = a S_{ut}^b \tag{6–19}$$

where S_{ut} is the minimum tensile strength and a and b are to be found in Table 6–2.

Surface Finish	Factor a		Exponent b
	S_{ut}, kpsi	S_{ut}, MPa	
Ground	1.34	1.58	−0.085
Machined or cold-drawn	2.70	4.51	−0.265
Hot-rolled	14.4	57.7	−0.718
As-forged	39.9	272.	−0.995

Size Factor k_b

The size factor has been evaluated using 133 sets of data points.[15] The results for bending and torsion may be expressed as

$$k_b = \begin{cases} (d/0.3)^{-0.107} = 0.879d^{-0.107} & 0.11 \leq d \leq 2 \text{ in} \\ 0.91d^{-0.157} & 2 < d \leq 10 \text{ in} \\ (d/7.62)^{-0.107} = 1.24d^{-0.107} & 2.79 \leq d \leq 51 \text{ mm} \\ 1.51d^{-0.157} & 51 < d \leq 254 \text{ mm} \end{cases} \tag{6–20}$$

For axial loading there is no size effect, so

$$k_b = 1 \tag{6–21}$$

EXAMPLE 6–4 A steel shaft loaded in bending is 52 mm in diameter, abutting a filleted shoulder 38 mm in diameter. The shaft material has a mean ultimate tensile strength of 690 MPa. Estimate the Marin size factor k_b if the shaft is used in

(*a*) A rotating mode.

(*b*) A nonrotating mode.

Solution (*a*) From Eq. (6–20)

Answer

$$k_b = 1.51d^{-0.157} = 1.51(52)^{-0.157} = 0.812$$

(*b*) From Table 6–3,

$$d_e = 0.37d = 0.37(52) = 19.24 \text{ mm}$$

From Eq. (6–20),

Answer

$$k_b = \left(\frac{19.24}{7.62}\right)^{-0.107} = 0.906$$

Common Nonrotating Structural Shapes

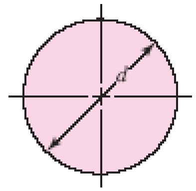

$$A_{0.95\sigma} = 0.01046d^2$$
$$d_e = 0.370d$$

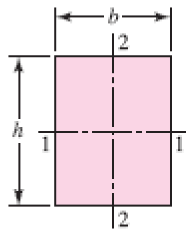

$$A_{0.95\sigma} = 0.05hb$$
$$d_e = 0.808\sqrt{hb}$$

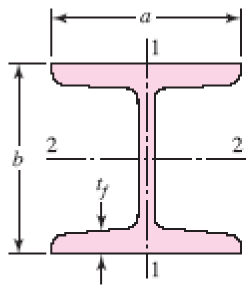

$$A_{0.95\sigma} = \begin{cases} 0.10at_f & \text{axis 1-1} \\ 0.05ba \quad t_f > 0.025a & \text{axis 2-2} \end{cases}$$

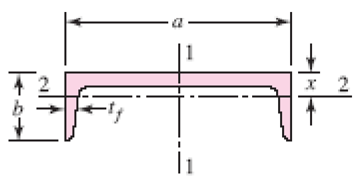

$$A_{0.95\sigma} = \begin{cases} 0.05ab & \text{axis 1-1} \\ 0.052xa + 0.1t_f(b-x) & \text{axis 2-2} \end{cases}$$

Loading Factor k_c

When fatigue tests are carried out with rotating bending, axial (push-pull), and torsional loading, the endurance limits differ with S_{ut}. This is discussed further in Sec. 6–17. Here, we will specify average values of the load factor as

$$k_c = \begin{cases} 1 & \text{bending} \\ 0.85 & \text{axial} \\ 0.59 & \text{torsion}^{17} \end{cases} \tag{6–26}$$

Temperature Factor k_d

Effect of Operating Temperature on the Tensile Strength of Steel.* (S_T = tensile strength at operating temperature; S_{RT} = tensile strength at room temperature; $0.099 \le \hat{\sigma} \le 0.110$)

Temperature, °C	S_T/S_{RT}	Temperature, °F	S_T/S_{RT}
20	1.000	70	1.000
50	1.010	100	1.008
100	1.020	200	1.020
150	1.025	300	1.024
200	1.020	400	1.018
250	1.000	500	0.995
300	0.975	600	0.963
350	0.943	700	0.927
400	0.900	800	0.872
450	0.843	900	0.797
500	0.768	1000	0.698
550	0.672	1100	0.567
600	0.549		

$$k_d = 0.975 + 0.432(10^{-3})T_F - 0.115(10^{-5})T_F^2 + 0.104(10^{-8})T_F^3 - 0.595(10^{-12})T_F^4 \tag{6–27}$$

where $70 \leq T_F \leq 1000°F$.

Two types of problems arise when temperature is a consideration. If the rotating-beam endurance limit is known at room temperature, then use

$$k_d = \frac{S_T}{S_{RT}} \tag{6–28}$$

from Table 6–4 or Eq. (6–27) and proceed as usual. If the rotating-beam endurance limit is not given, then compute it using Eq. (6–8) and the temperature-corrected tensile strength obtained by using the factor from Table 6–4. Then use $k_d = 1$.

EXAMPLE 6–5

A 1035 steel has a tensile strength of 490 MPa and is to be used for a part that sees 230°C in service. Estimate the Marin temperature modification factor and $(S_e)_{230°}$ if
(*a*) The room-temperature endurance limit by test is $(S'_e)_{37°} = 270$ MPa.
(*b*) Only the tensile strength at room temperature is known.

Solution

(*a*) First, from Eq. (6–27),

$$k_d = 0.9877 + 0.6507(10^{-3})(230) - 0.3414(10^{-5})(230^2) + 0.5621(10^{-8})(230^3) - 6.246(10^{-12})(230^4) = 1.00767$$

Thus,

Answer

$$(S_e)_{230°} = k_d\,(S'_e)_{37°} = 1.00767(270) = 272.07 \text{ MPa}$$

(*b*) Interpolating from Table 6–4 gives

$$(S_T)\,S_{RT})_{230°} = 1.02 + (1.0 - 1.02)\,\frac{230 - 200}{250 - 200} = 1.0197$$

Thus, the tensile strength at 230°C is estimated as

$$(S_{ut})_{230°} = (S_T\,/\,S_{RT})_{230°}\,(S_{ut})_{37°} = 1.0197(490) = 499.7 \text{ MPa}$$

From Eq. (6–8) then,

Answer

$$(S_e)_{230°} = 0.5(S_{ut})_{230°} = 0.5(499.7) = 249.9 \text{ MPa}$$

Part *a* gives the better estimate due to actual testing of the particular material.

Reliability Factor k_e

$$k_e = 1 - 0.08\, z_a \tag{6–29}$$

where z_a is defined by Eq. (20–16) and values for any desired reliability can be determined from Table A–10. Table 6–5 gives reliability factors for some standard specified reliabilities.

Reliability, %	Transformation Variate z_a	Reliability Factor k_e
50	0	1.000
90	1.288	0.897
95	1.645	0.868
99	2.326	0.814
99.9	3.091	0.753
99.99	3.719	0.702
99.999	4.265	0.659
99.9999	4.753	0.620

Miscellaneous-Effects Factor k_f

Though the factor k_f is intended to account for the reduction in endurance limit due to all other effects, it is really intended as a reminder that these must be accounted for, because actual values of k_f are not always available.

Residual stresses may either improve the endurance limit or affect it adversely. Generally, if the residual stress in the surface of the part is compression, the endurance limit is improved. Fatigue failures appear to be tensile failures, or at least to be caused by tensile stress, and so anything that reduces tensile stress will also reduce the possibility of a fatigue failure. Operations such as shot peening, hammering, and cold rolling build compressive stresses into the surface of the part and improve the endurance limit significantly. Of course, the material must not be worked to exhaustion.

The endurance limits of parts that are made from rolled or drawn sheets or bars, as well as parts that are forged, may be affected by the so-called *directional characteristics* of the operation. Rolled or drawn parts, for example, have an endurance limit in the transverse direction that may be 10 to 20 percent less than the endurance limit in the longitudinal direction.

Parts that are case-hardened may fail at the surface or at the maximum core radius, depending upon the stress gradient. Figure 6–19 shows the typical triangular stress distribution of a bar under bending or torsion. Also plotted as a heavy line in this figure are the endurance limits S_e for the case and core. For this example the endurance limit of the core rules the design because the figure shows that the stress σ or τ, whichever applies, at the outer core radius, is appreciably larger than the core endurance limit.

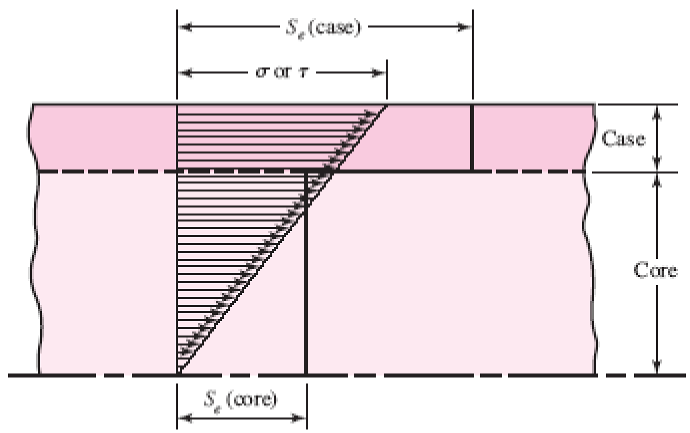

Corrosion

It is to be expected that parts that operate in a corrosive atmosphere will have a lowered fatigue resistance. This is, of course, true, and it is due to the roughening or pitting of the surface by the corrosive material. But the problem is not so simple as the one of finding the endurance limit of a specimen that has been corroded. The reason for this is that the corrosion and the stressing occur at the same time. Basically, this means that in time any part will fail when subjected to repeated stressing in a corrosive atmosphere. There is no fatigue limit. Thus the designer's problem is to attempt to minimize the factors that affect the fatigue life; these are:

- Mean or static stress
- Alternating stress
- Electrolyte concentration
- Dissolved oxygen in electrolyte
- Material properties and composition
- Temperature
- Cyclic frequency
- Fluid flow rate around specimen

Electrolytic Plating

Metallic coatings, such as chromium plating, nickel plating, or cadmium plating, reduce the endurance limit by as much as 50 percent. In some cases the reduction by coatings has been so severe that it has been necessary to eliminate the plating process. Zinc plating does not affect the fatigue strength. Anodic oxidation of light alloys reduces bending endurance limits by as much as 39 percent but has no effect on the torsional endurance limit.

Metal Spraying

Metal spraying results in surface imperfections that can initiate cracks. Limited tests show reductions of 14 percent in the fatigue strength.

Cyclic Frequency

If, for any reason, the fatigue process becomes time-dependent, then it also becomes frequency-dependent. Under normal conditions, fatigue failure is independent of frequency. But when corrosion or high temperatures, or both, are encountered, the cyclic rate becomes important. The slower the frequency and the higher the temperature, the higher the crack propagation rate and the shorter the life at a given stress level.

Frettage Corrosion

The phenomenon of frettage corrosion is the result of microscopic motions of tightly fitting parts or structures. Bolted joints, bearing-race fits, wheel hubs, and any set of tightly fitted parts are examples. The process involves surface discoloration, pitting, and eventual fatigue. The frettage factor k_f depends upon the material of the mating pairs and ranges from 0.24 to 0.90.

Stress Concentration

Any discontinuity in a machine part alters the

stress distribution in the neighborhood of the discontinuity so that the elementary stress equations no longer describe the state of stress in the part at these locations. Such discontinuities are called *stress raisers*, and the regions in which they occur are called areas of *stress concentration*.

A *theoretical*, or *geometric*, *stress-concentration factor* K_t or K_{ts} is used to relate the actual maximum stress at the discontinuity to the nominal stress. The factors are defined by the equations

$$K_t = \frac{\sigma_{max}}{\sigma_0} \qquad K_{ts} = \frac{\tau_{max}}{\tau_0} \tag{3–48}$$

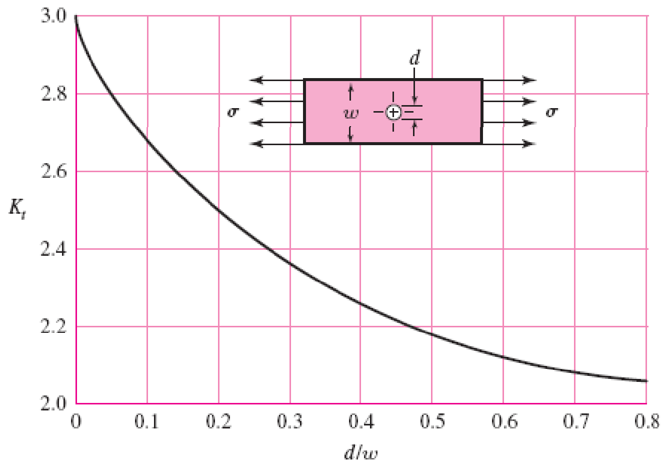

Figure A–15–1

Bar in tension or simple compression with a transverse hole. $\sigma_0 = F/A$, where $A = (w - d)t$ and t is the thickness.

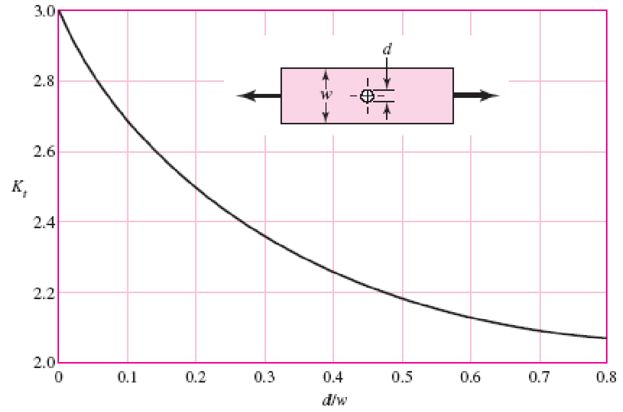

Figure A–15–2

Rectangular bar with a transverse hole in bending. $\sigma_0 = Mc/I$, where $I = (w - d)h^3/12$.

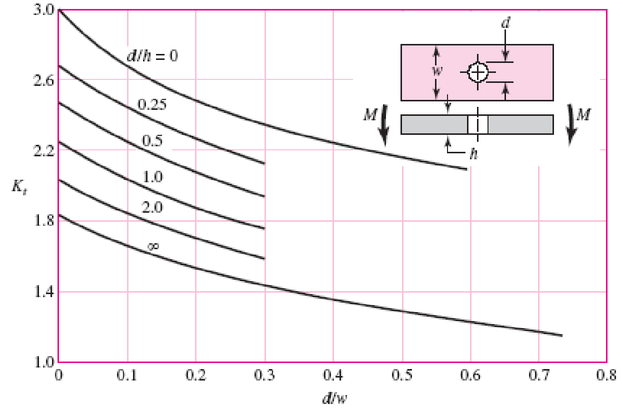

Figure A–15–3

Notched rectangular bar in tension or simple compression. $\sigma_0 = F/A$, where $A = dt$ and t is the thickness.

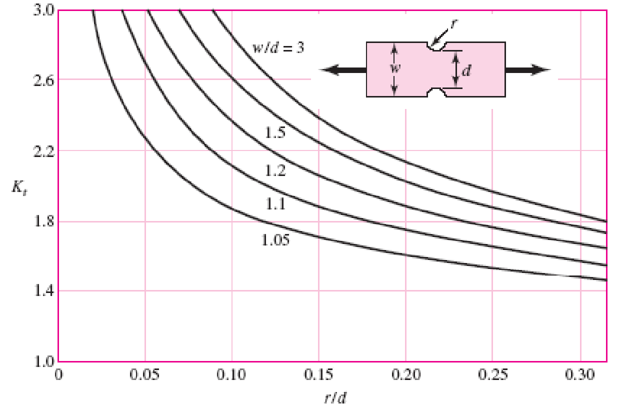

6–10 Stress Concentration and Notch Sensitivity

In Sec. 3–13 it was pointed out that the existence of irregularities or discontinuities, such as holes, grooves, or notches, in a part increases the theoretical stresses significantly in the immediate vicinity of the discontinuity. Equation (3–48) defined a stress concentration factor K_t (or K_{ts}), which is used with the nominal stress to obtain the maximum resulting stress due to the irregularity or defect. It turns out that some materials are not fully sensitive to the presence of notches and hence, for these, a reduced value of K_t can be used. For these materials, the maximum stress is, in fact,

$$\sigma_{\max} = K_f \sigma_0 \qquad \text{or} \qquad \tau_{\max} = K_{fs} \tau_0 \tag{6–30}$$

where K_f is a reduced value of K_t and σ_0 is the nominal stress. The factor K_f is commonly called a *fatigue stress-concentration factor,* and hence the subscript f. So it is convenient to think of K_f as a stress-concentration factor reduced from K_t because of lessened sensitivity to notches. The resulting factor is defined by the equation

$$K_f = \frac{\text{maximum stress in notched specimen}}{\text{stress in notch-free specimen}} \tag{a}$$

Notch sensitivity q is defined by the equation

$$q = \frac{K_f - 1}{K_t - 1} \qquad \text{or} \qquad q_{\text{shear}} = \frac{K_{fs} - 1}{K_{ts} - 1} \tag{6–31}$$

where q is usually between zero and unity. Equation (6–31) shows that if $q = 0$, then $K_f = 1$, and the material has no sensitivity to notches at all. On the other hand, if $q = 1$, then $K_f = K_t$, and the material has full notch sensitivity. In analysis or design work, find K_t first, from the geometry of the part. Then specify the material, find q, and solve for K_f from the equation

$$K_f = 1 + q(K_t - 1) \qquad \text{or} \qquad K_{fs} = 1 + q_{\text{shear}}(K_{ts} - 1) \tag{6–32}$$

For steels and 2024 aluminum alloys, use Fig. 6–20 to find q for bending and axial loading. For shear loading, use Fig. 6–21. In using these charts it is well to know that the actual test results from which the curves were derived exhibit a large amount of

about the true value of q. Also, note that q is not far from unity for large notch radii.

The notch sensitivity of the cast irons is very low, varying from 0 to about 0.20, depending upon the tensile strength. To be on the conservative side, it is recommended that the value $q = 0.20$ be used for all grades of cast iron.

Figure 6–20 has as its basis the *Neuber equation,* which is given by

$$K_f = 1 + \frac{K_t - 1}{1 + \sqrt{a/r}} \qquad (6\text{–}33)$$

where $\sqrt{a}$ is defined as the *Neuber constant* and is a material constant. Equating Eqs. (6–31) and (6–33) yields the notch sensitivity equation

$$q = \frac{1}{1 + \dfrac{\sqrt{a}}{\sqrt{r}}} \qquad (6\text{–}34)$$

For steel, with S_{ut} in *kpsi*, the Neuber constant can be approximated by a third-order polynomial fit of data as

$$\text{Bending or axial:} \quad \sqrt{a} = 0.246 - 3.08(10^{-3})S_{ut} + 1.51(10^{-5})S_{ut}^2 - 2.67(10^{-8})S_{ut}^3 \qquad (6\text{–}35a)$$

$$\text{Torsion:} \quad \sqrt{a} = 0.190 - 2.51(10^{-3})S_{ut} + 1.35(10^{-5})S_{ut}^2 - 2.67(10^{-8})S_{ut}^3 \qquad (6\text{–}35b)$$

To be conservative, it is recommended that the value of q = 0.2 for all grades of cast iron.

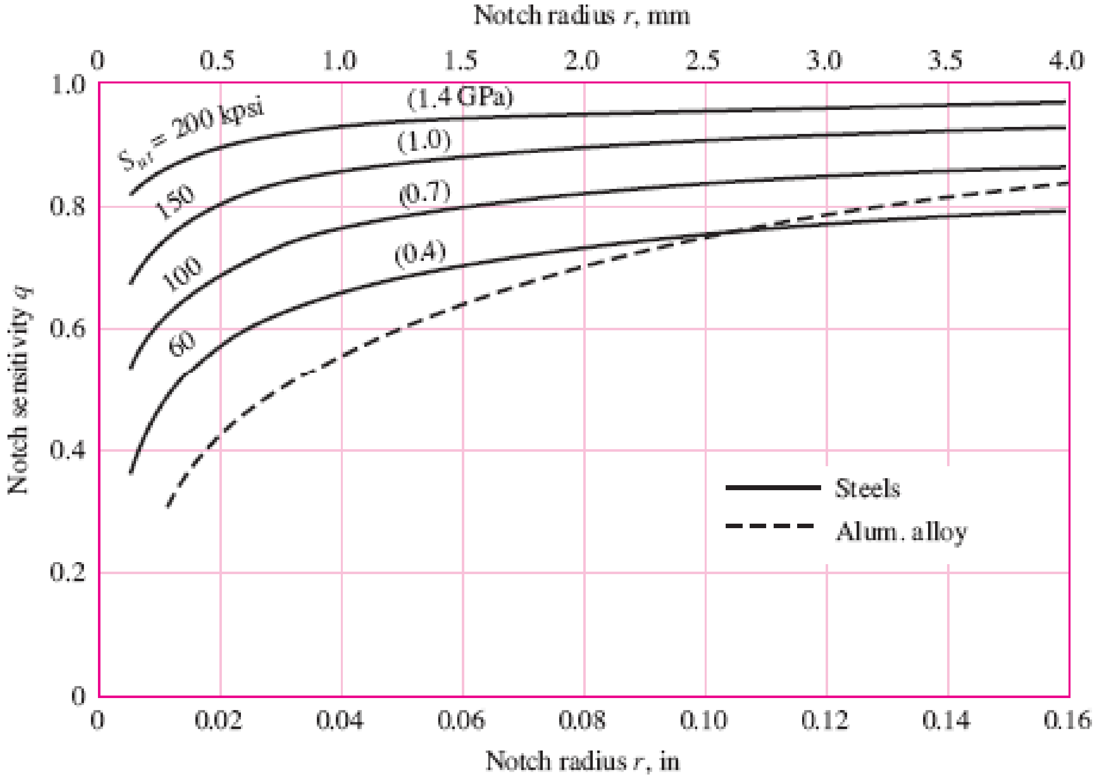

Figure 6–20

Notch-sensitivity charts for steels and UNS A92024-T wrought aluminum alloys subjected to reversed bending or reversed axial loads. For larger notch radii, use the values of q corresponding to the $r = 0.16$-in (4-mm) ordinate. *(From George Sines and J. L. Waisman (eds.),* Metal Fatigue, McGraw-Hill, New York. Copyright © 1969 by The McGraw-Hill Companies, Inc. Reprinted by permission.)

Figure 6–21

Notch-sensitivity curves for materials in reversed torsion. For larger notch radii, use the values of q_{shear} corresponding to $r = 0.16$ in (4 mm).

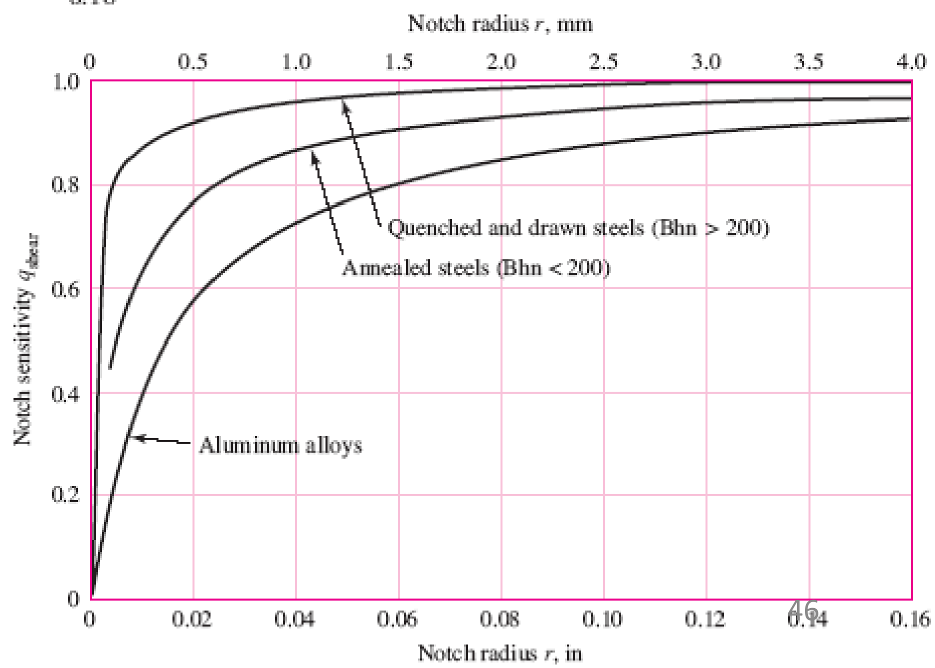

EXAMPLE 6–6 A steel shaft in bending has an ultimate strength of 690 MPa and a shoulder with a fillet radius of 3 mm connecting a 32-mm diameter with a 38-mm diameter. Estimate K_f using:

(*a*) Figure 6–20.

(*b*) Equations (6–33) and (6–35).

Solution From Fig. A–15–9, using $D/d = 38/32 = 1.1875$, $r/d = 3/32 = 0.093\,75$, we read the graph to find $K_t \doteq 1.65$.

(*a*) From Fig. 6–20, for $S_{ut} = 690$ MPa and $r = 3$ mm, $q \doteq 0.84$. Thus, from Eq. (6–32)

Answer

$$K_f = 1 + q(K_t - 1) \doteq 1 + 0.84(1.65 - 1) = 1.55$$

(*b*) From Eq. (6–35) with $S_{ut} = 690\text{ MPa} = 100\text{ kpsi}$, $\sqrt{a} = 0.0622\sqrt{\text{in}} = 0.313\sqrt{\text{mm}}$. Substituting this into Eq. (6–33) with $r = 3$ mm gives

Answer

$$K_f = 1 + \frac{K_t - 1}{1 + \sqrt{a/r}} \doteq 1 + \frac{1.65 - 1}{1 + \dfrac{0.313}{\sqrt{3}}} = 1.55$$

EXAMPLE 6–7 For the step-shaft of Ex. 6–6, it is determined that the fully corrected endurance limit is $S_e = 280$ MPa. Consider the shaft undergoes a fully reversing nominal stress in the fillet of $(\sigma_{\text{rev}})_{\text{nom}} = 260$ MPa. Estimate the number of cycles to failure.

Solution From Ex. 6–6, $K_f = 1.55$, and the ultimate strength is $S_{ut} = 690 \text{ MPa} = 100$ kpsi. The maximum reversing stress is

$$(\sigma_{\text{rev}})_{\text{max}} = K_f(\sigma_{\text{rev}})_{\text{nom}} = 1.55(260) = 403 \text{ MPa}$$

From Fig. 6–18, $f = 0.845$. From Eqs. (6–14), (6–15), and (6–16)

$$a = \frac{(f S_{ut})^2}{S_e} = \frac{[0.845(690)]^2}{280} = 1214 \text{ MPa}$$

$$b = -\frac{1}{3}\log\frac{f S_{ut}}{S_e} = -\frac{1}{3}\log\left[\frac{0.845(690)}{280}\right] = -0.1062$$

Answer

$$N = \left(\frac{\sigma_{\text{rev}}}{a}\right)^{1/b} = \left(\frac{403}{1214}\right)^{1/-0.1062} = 32.3(10^3) \text{ cycles}$$

Table A–20

Deterministic ASTM Minimum Tensile and Yield Strengths for Some Hot-Rolled (HR) and Cold-Drawn (CD) Steels [The strengths listed are estimated ASTM minimum values in the size range 18 to 32 mm ($\frac{3}{4}$ to $1\frac{1}{4}$ in). These strengths are suitable for use with the design factor defined in Sec. 1–10, provided the materials conform to ASTM A6 or A568 requirements or are required in the purchase specifications. Remember that a numbering system is not a specification.] Source: 1986 SAE Handbook, p. 2.15.

1 UNS No.	2 SAE and/or AISI No.	3 Processing	4 Tensile Strength, MPa (kpsi)	5 Yield Strength, MPa (kpsi)	6 Elongation in 2 in, %	7 Reduction in Area, %	8 Brinell Hardness
G10060	1006	HR	300 (43)	170 (24)	30	55	86
		CD	330 (48)	280 (41)	20	45	95
G10100	1010	HR	320 (47)	180 (26)	28	50	95
		CD	370 (53)	300 (44)	20	40	105
G10150	1015	HR	340 (50)	190 (27.5)	28	50	101
		CD	390 (56)	320 (47)	18	40	111
G10180	1018	HR	400 (58)	220 (32)	25	50	116
		CD	440 (64)	370 (54)	15	40	126
G10200	1020	HR	380 (55)	210 (30)	25	50	111
		CD	470 (68)	390 (57)	15	40	131
G10300	1030	HR	470 (68)	260 (37.5)	20	42	137
		CD	520 (76)	440 (64)	12	35	149
G10350	1035	HR	500 (72)	270 (39.5)	18	40	143
		CD	550 (80)	460 (67)	12	35	163
G10400	1040	HR	520 (76)	290 (42)	18	40	149
		CD	590 (85)	490 (71)	12	35	170
G10450	1045	HR	570 (82)	310 (45)	16	40	163
		CD	630 (91)	530 (77)	12	35	179
G10500	1050	HR	620 (90)	340 (49.5)	15	35	179
		CD	690 (100)	580 (84)	10	30	197
G10600	1060	HR	680 (98)	370 (54)	12	30	201
G10800	1080	HR	770 (112)	420 (61.5)	10	25	229
G10950	1095	HR	830 (120)	460 (66)	10	25	248

EXAMPLE 6–8 A 1015 hot-rolled steel bar has been machined to a diameter of 25 mm. It is to be placed in reversed axial loading for 70 000 cycles to failure in an operating environment of 300°C. Using ASTM minimum properties, and a reliability of 99 percent, estimate the endurance limit and fatigue strength at 70 000 cycles.

Solution From Table A–20, $S_{ut} = 340$ MPa at 20°C. Since the rotating-beam specimen endurance limit is not known at room temperature, we determine the ultimate strength at the elevated temperature first, using Table 6–4. From Table 6–4,

$$\left(\frac{S_T}{S_{RT}}\right)_{300^\circ} = 0.975$$

The ultimate strength at 300°C is then

$$(S_{ut})_{300^\circ} = (S_T\,/\,S_{RT})_{300^\circ}\,(S_{ut})_{20^\circ} = 0.975(340) = 331.5 \text{ MPa}$$

The rotating-beam specimen endurance limit at 300°C is then estimated from Eq. (6–8) as

$$S'_e = 0.5(331.5) = 165.8 \text{ MPa}$$

Next, we determine the Marin factors. For the machined surface, Eq. (6–19) with Table 6–2 gives

$$k_a = aS_{ut}^b = 4.51(331.5^{-0.265}) = 0.969$$

For axial loading, from Eq. (6–21), the size factor $k_b = 1$, and from Eq. (6–26) the loading factor is $k_c = 0.85$. The temperature factor $k_d = 1$, since we accounted for the temperature in modifying the ultimate strength and consequently the endurance limit. For 99 percent reliability, from Table 6–5, $k_e = 0.814$. Finally, since no other conditions were given, the miscellaneous factor is $k_f = 1$. The endurance limit for the part is estimated by Eq. (6–18) as

Answer

$$\begin{aligned} S_e &= k_a k_b k_c k_d k_e k_f S'_e \\ &= 0.969(1)(0.85)(1)(0.814)(1)165.8 = 111 \text{ MPa} \end{aligned}$$

For the fatigue strength at 70 000 cycles we need to construct the *S-N* equation. From p. 285, since $S_{ut} = 331.5 < 490$ MPa, then $f = 0.9$. From Eq. (6–14)

$$a = \frac{(f\,S_{ut})^2}{S_e} = \frac{[0.9(331.5)]^2}{111} = 891 \text{ MPa}$$

and Eq. (6–15)

$$b = -\frac{1}{3}\log\left(\frac{f\ S_{ut}}{S_e}\right) = -\frac{1}{3}\log\left[\frac{0.9(331.5)}{111}\right] = -0.1431$$

Finally, for the fatigue strength at 70 000 cycles, Eq. (6–13) gives

Answer

$$S_f = a\ N^b = 891(70\,000)^{-0.1431} = 180.5 \text{ MPa}$$

EXAMPLE 6–9 Figure 6–22*a* shows a rotating shaft simply supported in ball bearings at A and D and loaded by a nonrotating force F of 6.8 kN. Using ASTM "minimum" strengths, estimate the life of the part.

Solution From Fig. 6–22*b* we learn that failure will probably occur at B rather than at C or at the point of maximum moment. Point B has a smaller cross section, a higher bending moment, and a higher stress-concentration factor than C, and the location of maximum moment has a larger size and no stress-concentration factor.

We shall solve the problem by first estimating the strength at point B, since the strength will be different elsewhere, and comparing this strength with the stress at the same point.

From Table A–20 we find $S_{ut} = 690$ MPa and $S_y = 580$ MPa. The endurance limit S'_e is estimated as

$$S'_e = 0.5(690) = 345 \text{ MPa}$$

From Eq. (6–19) and Table 6–2,

$$k_a = 4.51(690)^{-0.265} = 0.798$$

From Eq. (6–20),

$$k_b = (32/7.62)^{-0.107} = 0.858$$

Since $k_c = k_d = k_e = k_f = 1$,

$$S_e = 0.798(0.858)345 = 236 \text{ MPa}$$

To find the geometric stress-concentration factor K_t we enter Fig. A–15–9 with $D/d = 38/32 = 1.1875$ and $r/d = 3/32 = 0.093\,75$ and read $K_t \doteq 1.65$. Substituting $S_{ut} = 690/6.89 = 100$ kpsi into Eq. (6–35) yields $\sqrt{a} = 0.0622\sqrt{\text{in}} = 0.313\sqrt{\text{mm}}$. Substituting this into Eq. (6–33) gives

$$K_f = 1 + \frac{K_t - 1}{1 + \sqrt{a/r}} = 1 + \frac{1.65 - 1}{1 + 0.313/\sqrt{3}} = 1.55$$

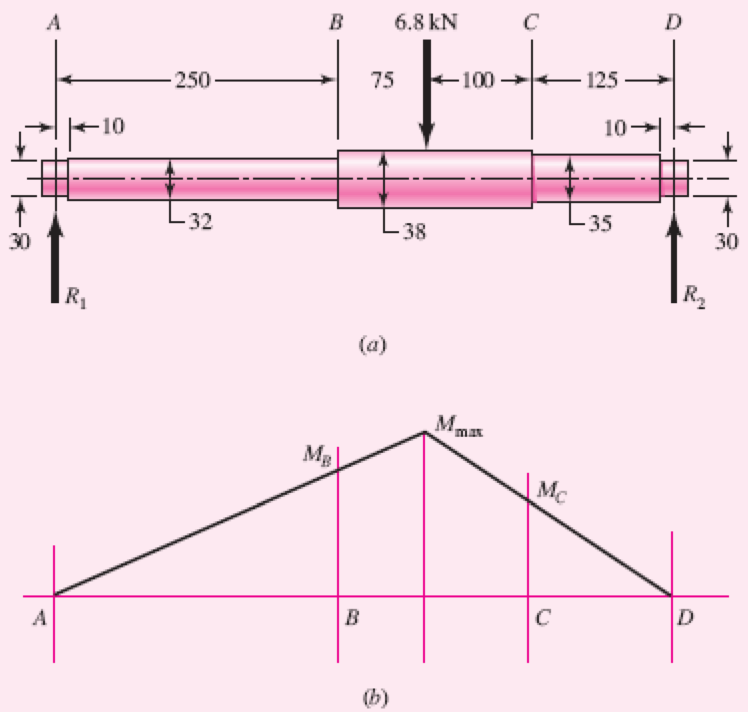

Figure 6–22

(*a*) Shaft drawing showing all dimensions in millimeters; all fillets 3-mm radius. The shaft rotates and the load is stationary; material is machined from AISI 1050 cold-drawn steel. (*b*) Bending-moment diagram.

The next step is to estimate the bending stress at point B. The bending moment is

$$M_B = R_1 x = \frac{225F}{550}250 = \frac{225(6.8)}{550}250 = 695.5\ \text{N}\cdot\text{m}$$

Just to the left of B the section modulus is $I/c = \pi d^3/32 = \pi 32^3/32 = 3.217\ (10^3)\text{mm}^3$. The reversing bending stress is, assuming infinite life,

$$\sigma = K_f \frac{M_B}{I/c} = 1.55\frac{695.5}{3.217}(10)^{-6} = 335.1(10^6)\ \text{Pa} = 335.1\ \text{MPa}$$

This stress is greater than S_e and less than S_y. This means we have both finite life and no yielding on the first cycle.

For finite life, we will need to use Eq. (6–16). The ultimate strength, $S_{ut} = 690$ MPa = 100 kpsi. From Fig. 6–18, $f = 0.844$. From Eq. (6–14)

$$a = \frac{(f\ S_{ut})^2}{S_e} = \frac{[0.844(690)]^2}{236} = 1437\ \text{MPa}$$

and from Eq. (6–15)

$$b = -\frac{1}{3}\log\left(\frac{f\ S_{ut}}{S_e}\right) = -\frac{1}{3}\log\left[\frac{0.844(690)}{236}\right] = -0.1308$$

From Eq. (6–16),

Answer $$N = \left(\frac{\sigma_a}{a}\right)^{1/b} = \left(\frac{335.1}{1437}\right)^{-1/0.1308} = 68(10^3)\ \text{cycles}$$

6–12 Fatigue Failure Criteria for Fluctuating Stress

Figure 6–27

Fatigue diagram showing various criteria of failure. For each criterion, points on or "above" the respective line indicate failure. Some point A on the Goodman line, for example, gives the strength S_m as the limiting value of σ_m corresponding to the strength S_a, which, paired with σ_m, is the limiting value of σ_a.

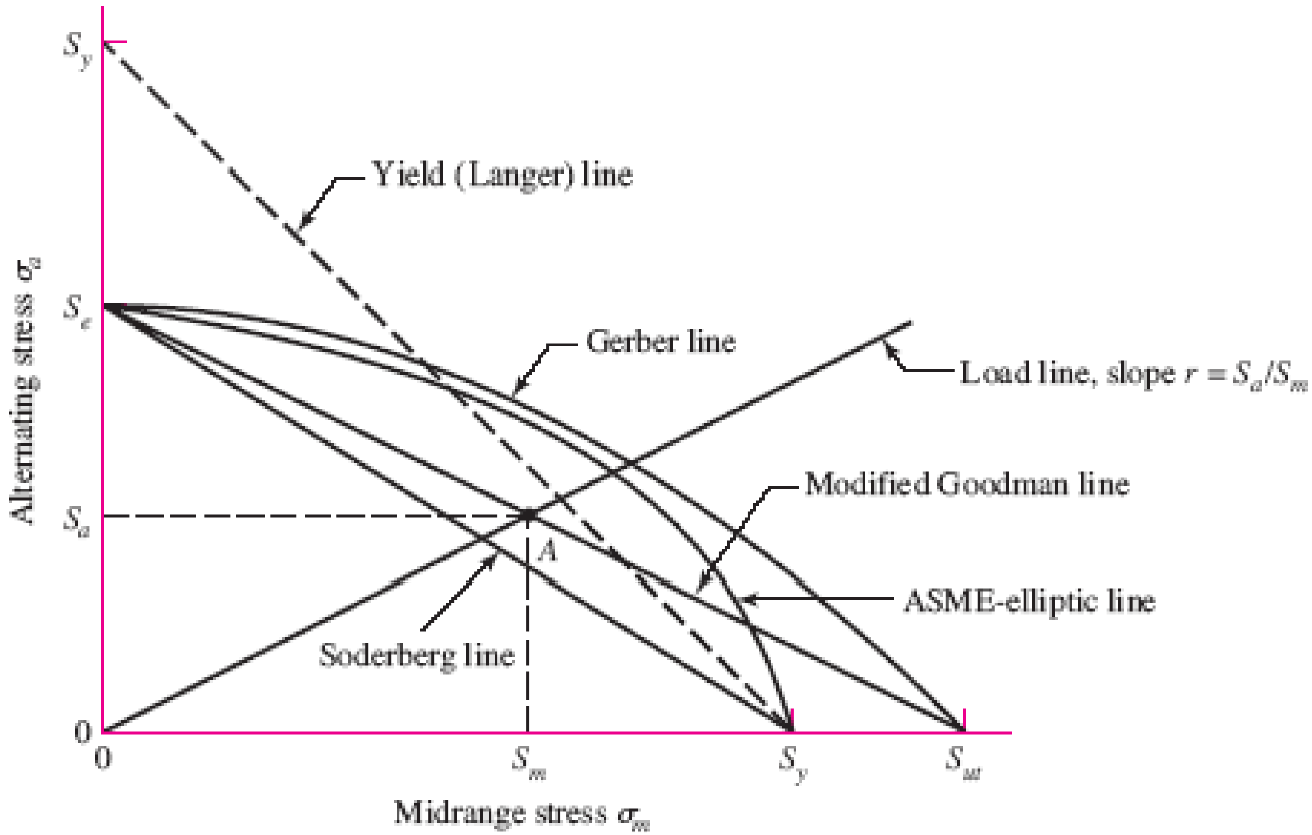

Five criteria of failure are diagrammed in Fig. 6–27: the Soderberg, the modified Goodman, the Gerber, the ASME-elliptic, and yielding. The diagram shows that only the Soderberg criterion guards against any yielding, but is biased low.

The criterion equation for the Soderberg line is

$$\frac{S_a}{S_e} + \frac{S_m}{S_y} = 1 \qquad (6\text{–}40)$$

Similarly, we find the modified Goodman relation to be

$$\frac{S_a}{S_e} + \frac{S_m}{S_{ut}} = 1 \qquad (6\text{–}41)$$

Examination of Fig. 6–25 shows that both a parabola and an ellipse have a better opportunity to pass among the midrange tension data and to permit quantification of the probability of failure. The Gerber failure criterion is written as

$$\frac{S_a}{S_e} + \left(\frac{S_m}{S_{ut}}\right)^2 = 1 \qquad (6\text{–}42)$$

and the ASME-elliptic is written as

$$\left(\frac{S_a}{S_e}\right)^2 + \left(\frac{S_m}{S_y}\right)^2 = 1 \qquad (6\text{–}43)$$

The *Langer* first-cycle-yielding criterion is used in connection with the fatigue curve:

$$S_a + S_m = S_y \qquad (6\text{–}44)$$

The stresses $n\sigma_a$ and $n\sigma_m$ can replace S_a and S_m, where n is the design factor or factor of safety. Then, Eq. (6–40), the Soderberg line, becomes

$$\textbf{Soderberg} \quad \frac{\sigma_a}{S_e} + \frac{\sigma_m}{S_y} = \frac{1}{n} \tag{6–45}$$

Equation (6–41), the modified Goodman line, becomes

$$\textbf{mod-Goodman} \quad \frac{\sigma_a}{S_e} + \frac{\sigma_m}{S_{ut}} = \frac{1}{n} \tag{6–46}$$

Equation (6–42), the Gerber line, becomes

$$\textbf{Gerber} \quad \frac{n\sigma_a}{S_e} + \left(\frac{n\sigma_m}{S_{ut}}\right)^2 = 1 \tag{6–47}$$

Equation (6–43), the ASME-elliptic line, becomes

$$\textbf{ASME-elliptic} \quad \left(\frac{n\sigma_a}{S_e}\right)^2 + \left(\frac{n\sigma_m}{S_y}\right)^2 = 1 \tag{6–48}$$

$$\textbf{Langer static yield} \quad \sigma_a + \sigma_m = \frac{S_y}{n}$$

The failure criteria are used in conjunction with a load line, $r = S_a/S_m = \sigma_a/\sigma_m$. Principal intersections are tabulated in Tables 6–6 to 6–8. Formal expressions for fatigue factor of safety are given in the lower panel of Tables 6–6 to 6–8. The first row of each table corresponds to the fatigue criterion, the second row is the static Langer criterion, and the third row corresponds to the intersection of the static and fatigue

Table 6–6

Amplitude and Steady Coordinates of Strength and Important Intersections in First Quadrant for Modified Goodman and Langer Failure Criteria

Intersecting Equations	Intersection Coordinates
$\dfrac{S_a}{S_e} + \dfrac{S_m}{S_{ut}} = 1$ Load line $r = \dfrac{S_a}{S_m}$	$S_a = \dfrac{r\,S_e S_{ut}}{r\,S_{ut} + S_e}$ $S_m = \dfrac{S_a}{r}$
$\dfrac{S_a}{S_y} + \dfrac{S_m}{S_y} = 1$ Load line $r = \dfrac{S_a}{S_m}$	$S_a = \dfrac{r\,S_y}{1+r}$ $S_m = \dfrac{S_y}{1+r}$
$\dfrac{S_a}{S_e} + \dfrac{S_m}{S_{ut}} = 1$ $\dfrac{S_a}{S_y} + \dfrac{S_m}{S_y} = 1$	$S_m = \dfrac{(S_y - S_e)\,S_{ut}}{S_{ut} - S_e}$ $S_a = S_y - S_m,\ r_{crit} = S_a/S_m$

Fatigue factor of safety

$$n_f = \frac{1}{\dfrac{\sigma_a}{S_e} + \dfrac{\sigma_m}{S_{ut}}}$$

Table 6–8

Amplitude and Steady Coordinates of Strength and Important Intersections in First Quadrant for ASME-Elliptic and Langer Failure Criteria

Intersecting Equations	Intersection Coordinates
$\left(\frac{S_a}{S_e}\right)^2 + \left(\frac{S_m}{S_y}\right)^2 = 1$	$S_a = \sqrt{\frac{r^2 S_e^2 S_y^2}{S_e^2 + r^2 S_y^2}}$
Load line $r = S_a / S_m$	$S_m = \frac{S_a}{r}$
$\frac{S_a}{S_y} + \frac{S_m}{S_y} = 1$	$S_a = \frac{r S_y}{1+r}$
Load line $r = S_a / S_m$	$S_m = \frac{S_y}{1+r}$
$\left(\frac{S_a}{S_e}\right)^2 + \left(\frac{S_m}{S_y}\right)^2 = 1$	$S_a = 0, \ \frac{2 S_y S_e^2}{S_e^2 + S_y^2}$
$\frac{S_a}{S_y} + \frac{S_m}{S_y} = 1$	$S_m = S_y - S_a, \ r_{crit} = S_a / S_m$

Fatigue factor of safety

$$n_f = \sqrt{\frac{1}{(\sigma_a / S_e)^2 + (\sigma_m / S_y)^2}}$$

Table 6–7

Amplitude and Steady Coordinates of Strength and Important Intersections in First Quadrant for Gerber and Langer Failure Criteria

Intersecting Equations	Intersection Coordinates
$\frac{S_a}{S_e} + \left(\frac{S_m}{S_{ut}}\right)^2 = 1$	$S_a = \frac{r^2 S_{ut}^2}{2S_e}\left[-1 + \sqrt{1 + \left(\frac{2S_e}{r S_{ut}}\right)^2}\,\right]$
Load line $r = \frac{S_a}{S_m}$	$S_m = \frac{S_a}{r}$
$\frac{S_a}{S_y} + \frac{S_m}{S_y} = 1$	$S_a = \frac{r S_y}{1 + r}$
Load line $r = \frac{S_a}{S_m}$	$S_m = \frac{S_y}{1 + r}$
$\frac{S_a}{S_e} + \left(\frac{S_m}{S_{ut}}\right)^2 = 1$	$S_m = \frac{S_{ut}^2}{2S_e}\left[1 - \sqrt{1 + \left(\frac{2S_e}{S_{ut}}\right)^2 \left(1 - \frac{S_y}{S_e}\right)}\,\right]$
$\frac{S_a}{S_y} + \frac{S_m}{S_y} = 1$	$S_a = S_y - S_m,\ r_{crit} = S_a / S_m$

Fatigue factor of safety

$$n_f = \frac{1}{2}\left(\frac{S_{ut}}{\sigma_m}\right)^2 \frac{\sigma_a}{S_e}\left[-1 + \sqrt{1 + \left(\frac{2\sigma_m S_e}{S_{ut}\sigma_a}\right)^2}\,\right] \qquad \sigma_m > 0$$

EXAMPLE 6–10 A 40-mm-diameter bar has been machined from an AISI 1050 cold-drawn bar. This part is to withstand a fluctuating tensile load varying from 0 to 70 kN. Because of the ends, and the fillet radius, a fatigue stress-concentration factor K_f is 1.85 for 10^6 or larger life. Find S_a and S_m and the factor of safety guarding against fatigue and first-cycle yielding, using (*a*) the Gerber fatigue line and (*b*) the ASME-elliptic fatigue line.

Solution We begin with some preliminaries. From Table A–20, $S_{ut} = 690$ MPa and $S_y = 580$ MPa. Note that $F_a = F_m = 35$ kN. The Marin factors are, deterministically,

$k_a = 4.51(690)^{-0.265} = 0.798$: Eq. (6–19), Table 6–2, p. 288

$k_b = 1$ (axial loading, see k_c)

$k_c = 0.85$: Eq. (6–26), p. 290

$k_d = k_e = k_f = 1$

$S_e = 0.798(1)0.850(1)(1)(1)0.5(690) = 234$ MPa: Eqs. (6–8), (6–18), p. 282, p. 287

The nominal axial stress components σ_{ao} and σ_{mo} are

$$\sigma_{ao} = \frac{4F_a}{\pi d^2} = \frac{4(35000)}{\pi\ 0.04^2} = 27.9\ <\text{Pa} \qquad \sigma_{mo} = \frac{4F_m}{\pi d^2} = \frac{4(35000)}{\pi\ 0.04^2} = 27.9\ <\text{Pa}$$

Applying K_f to both components σ_{ao} and σ_{mo} constitutes a prescription of no notch yielding:

$$\sigma_a = K_f \sigma_{ao} = 1.85(27.9) = 51.6\text{ MPa} = \sigma_m$$

(*a*) Let us calculate the factors of safety first. From the bottom panel from Table 6–7 the factor of safety for fatigue is

Answer
$$n_f = \frac{1}{2}\left(\frac{690}{51.5}\right)^2 \left(\frac{51.9}{234}\right)\left\{-1 + \sqrt{1 + \left[\frac{2(51.6)234}{690(51.6)}\right]^2}\right\} = 4.13$$

From Eq. (6–49) the factor of safety guarding against first-cycle yield is

Answer
$$n_y = \frac{S_y}{\sigma_a + \sigma_m} = \frac{580}{51.6 + 51.6} = 5.62$$

Thus, we see that fatigue will occur first and the factor of safety is 4.13. This can be seen in Fig. 6–28 where the load line intersects the Gerber fatigue curve first at point B. If the plots are created to true scale it would be seen that $n_f = OB/OA$.

From the first panel of Table 6–7, $r = \sigma_a/\sigma_m = 1$,

Answer
$$S_a = \frac{(1)^2\, 690^2}{2(234)}\left\{-1 + \sqrt{1 + \left[\frac{2(234)}{(1)690}\right]^2}\right\} = 211.9\text{ MPa}$$

Figure 6–28

Principal points A, B, C, and D on the designer's diagram drawn for Gerber, Langer, and load line.

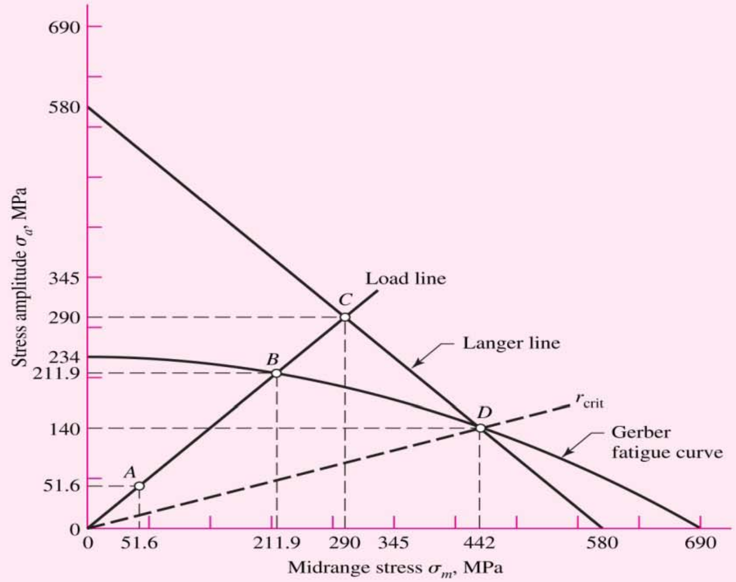

Answer

$$S_m = \frac{S_a}{r} = \frac{211.9}{1} = 211.9 \text{ MPa}$$

As a check on the previous result, $n_f = OB/OA = S_a/\sigma_a = S_m/\sigma_m = 211.9/51.6 = 4.12$ and we see total agreement.

We could have detected that fatigue failure would occur first without drawing Fig. 6–28 by calculating r_{crit}. From the third row third column panel of Table 6–7, the intersection point between fatigue and first-cycle yield is

$$S_m = \frac{690^2}{2(234)}\left[1 - \sqrt{1 + \left(\frac{2(234)}{690}\right)^2\left(1 - \frac{580}{234}\right)}\right] = 442 \text{ MPa}$$

$$S_a = S_y - S_m = 580 - 442 = 138 \text{ MPa}$$

The critical slope is thus

$$r_{\text{crit}} = \frac{S_a}{S_m} = \frac{138}{442} = 0.312$$

which is less than the actual load line of $r = 1$. This indicates that fatigue occurs before first-cycle-yield.

(b) Repeating the same procedure for the ASME-elliptic line, for fatigue

Answer

$$n_f = \sqrt{\frac{1}{(51.6/234)^2 + (51.6/580)^2}} = 4.21$$

Again, this is less than $n_y = 5.62$ and fatigue is predicted to occur first. From the first row second column panel of Table 6–8, with $r = 1$, we obtain the coordinates S_a and S_m of point B in Fig. 6–29 as

Figure 6–29

Principal points A, B, C, and D on the designer's diagram drawn for ASME-elliptic, Langer, and load lines.

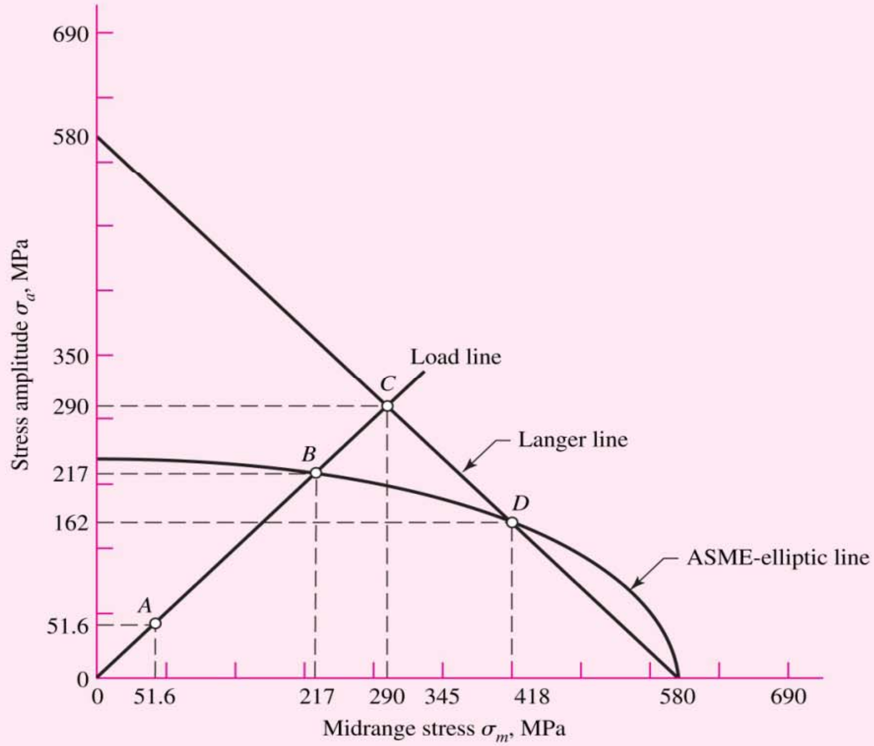

Answer

$$S_a = \sqrt{\frac{(1)^2 234^2 (580)^2}{234^2 + (1)^2 580^2}} = 217 \text{ MPa}, \quad S_m = \frac{S_a}{r} = \frac{217}{1} = 217 \text{ MPa}$$

To verify the fatigue factor of safety, $n_f = S_a/\sigma_a = 217/51.6 = 4.21$.

As before, let us calculate r_{crit}. From the third row second column panel of Table 6–8,

$$S_a = \frac{2(580)234^2}{234^2 + 580^2} = 162 \text{ MPa}, \quad S_m = S_y - S_a = 580 - 162 = 418 \text{ MPa}$$

$$r_{\text{crit}} = \frac{S_a}{S_m} = \frac{162}{418} = 0.388$$

which again is less than $r = 1$, verifying that fatigue occurs first with $n_f = 4.21$.

The Gerber and the ASME-elliptic fatigue failure criteria are very close to each other and are used interchangeably. The ANSI/ASME Standard B106.1M–1985 uses ASME-elliptic for shafting.

EXAMPLE 6–11 A flat-leaf spring is used to retain an oscillating flat-faced follower in contact with a plate cam. The follower range of motion is 50 mm and fixed, so the alternating component of force, bending moment, and stress is fixed, too. The spring is preloaded to adjust to various cam speeds. The preload must be increased to prevent follower float or jump. For lower speeds the preload should be decreased to obtain longer life of cam and follower surfaces. The spring is a steel cantilever 0.8 m long, 50 mm wide, and 6 mm thick, as seen in Fig. 6–30*a*. The spring strengths are $S_{ut} = 1000$ MPa, $S_y = 880$ MPa, and $S_e =$ 195 MPa fully corrected. The total cam motion is 50 mm. The designer wishes to preload the spring by deflecting it 50 mm for low speed and 125 mm for high speed.

(*a*) Plot the Gerber-Langer failure lines with the load line.

(*b*) What are the strength factors of safety corresponding to 50 mm and 125 mm preload?

Solution We begin with preliminaries. The second area moment of the cantilever cross section is

$$I = \frac{bh^3}{12} = \frac{0.05(0.006)^3}{12} = 0.9 + 10^{-9}\ \text{m}^4$$

Since, from Table A–9, beam 1, force F and deflection y in a cantilever are related by $F = 3EIy/l^3$, then stress σ and deflection y are related by

$$\sigma = \frac{Mc}{I} = \frac{0.8Fc}{I} = \frac{0.8(3EIy)}{l^3}\frac{c}{I} = \frac{2.4Ecy}{l^3} = Ky$$

$$\text{where } K = \frac{2.4Ec}{l^3} = \frac{2.4(210\times 10^9)(0.003)}{0.8^3} = 2.95\ \text{GPa/m}$$

Now the minimums and maximums of y and σ can be defined by

$$y_{\text{min}} = \delta \qquad y_{\text{max}} = 0.05 + \delta$$

$$\sigma_{\text{min}} = K\delta \qquad \sigma_{\text{max}} = K(0.05 + \delta)$$

Figure 6–30

Cam follower retaining spring. (*a*) Geometry; (*b*) designer's fatigue diagram for Ex. 6–11.

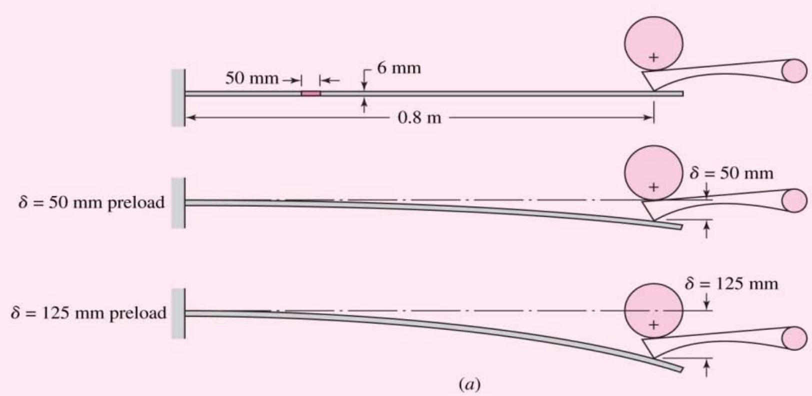

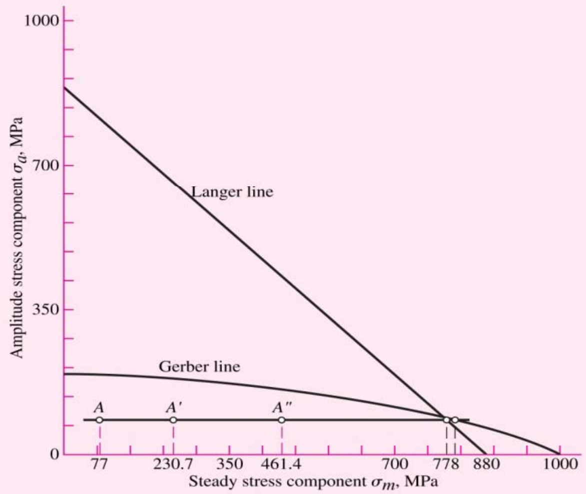

(*b*)

The stress components are thus

$$\sigma_a = \frac{K(0.05 + \delta) - K\delta}{0.05} = K = 76.9 \text{ MPa}$$

$$\sigma_m = \frac{K(0.05 + \delta) + K\delta}{0.05} = K(1 + 40\delta) = 76.9(1 + 40\delta)$$

For $\delta = 0$, $\quad \sigma_a = \sigma_m = 76.9 = 77$ MPa

For $\delta = 50$ mm, $\quad \sigma_a = 77$ MPa, $\sigma_m = 76.9[1 + 40(0.05)] = 230.7$ MPa

For $\delta = 125$ mm, $\quad \sigma_a = 77$ MPa, $\sigma_m = 76.9[1 + 40(0.125)] = 461.4$ MPa

(*a*) A plot of the Gerber and Langer criteria is shown in Fig. 6–30*b*. The three preload deflections of 0, 50, and 125 mm are shown as points A, A', and A''. Note that since σ_a is constant at 77 MPa, the load line is horizontal and does not contain the origin. The intersection between the Gerber line and the load line is found from solving Eq. (6–42) for S_m and substituting 77 MPa for S_a:

$$S_m = S_{ut}\sqrt{1 - \frac{S_a}{S_e}} = 1000\sqrt{1 - \frac{77}{195}} = 778 \text{ MPa}$$

The intersection of the Langer line and the load line is found from solving Eq. (6–44) for S_m and substituting 77 MPa for S_a:

$$S_m = S_y - S_a = 880 - 77 = 803 \text{ MPa}$$

The threats from fatigue and first-cycle yielding are approximately equal.

(*b*) For $\delta = 50$ mm,

Answer $$n_f = \frac{S_m}{\sigma_m} = \frac{778}{230.7} = 3.37 \qquad n_y = \frac{803}{230.7} = 3.48$$

and for $\delta = 125$ mm,

Answer $$n_f = \frac{778}{461.4} = 1.69 \qquad n_y = \frac{803}{461.4} = 1.74$$

EXAMPLE 6–12 Figure 6–31 shows a formed round-wire cantilever spring subjected to a varying force. The hardness tests made on 25 springs gave a minimum hardness of 380 Brinell. It is apparent from the mounting details that there is no stress concentration. A visual inspection of the springs indicates that the surface finish corresponds closely to a hot-rolled finish. What number of applications is likely to cause failure? Solve using:

(*a*) Modified Goodman criterion.

(*b*) Gerber criterion.

Solution

$$S_{ut} = 3.41(380) = 1295.8 \text{ MPa}$$

$$S_e' = 0.5(1295.8) = 648 \text{ MPa}$$

$$k_a = 57.7(1295.8)^{-0.718} = 0.336$$

For a non-rotating round bar in bending, Eq. (6–24) gives: $d_e = 0.370d = 0.370(10) =$ 3.7 mm

$$k_b = \left(\frac{3.7}{7.62}\right)^{-0.107} = 1.08$$

$$S_e = 0.336(1.08)(648) = 235 \text{ MPa}$$

$$F_a = \frac{120 - 60}{2} = 30 \text{ N}, \quad F_m = \frac{120 + 60}{2} = 90 \text{ N},$$

$$\sigma_m = \frac{32M_m}{\pi d^3} = \frac{32(90)(400)}{\pi(10^3)} = 366.7 \text{ MPa}$$

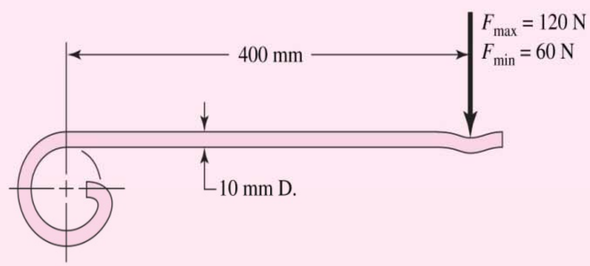

Figure 6–31

$$\sigma_a = \frac{32(30)(400)}{\pi(10^3)} = 122.2 \text{ MPa}$$

$$r = \frac{122.2}{366.7} = 0.333$$

(*a*) Modified Goodman, Table 6–6

$$n_f = \frac{1}{(122.2/235) + (366.7/1295.8)} = 1.25$$

From Fig. 6–18, for $S_{ut} = 1295.8$ MPa, $f = 0.78$

Eq. (6–14): $$a = \frac{[0.78(1295.8)]^2}{235} = 5573 \text{ MPa}$$

Eq. (6–15): $$b = -\frac{1}{3}\log\frac{0.78(1295.8)}{235} = -0.211\,19$$

$$\frac{\sigma_a}{S_f} + \frac{\sigma_m}{S_{ut}} = 1 \quad \Rightarrow \quad S_f = \frac{\sigma_a}{1 - (\sigma_m/S_{ut})} = \frac{122.2}{1 - (366.7/1295.8)} = 170.4 \text{ MPa}$$

Eq. (6–16) with $\sigma_a = S_f$

Answer
$$N = \left(\frac{170.4}{5573}\right)^{1/-0.211\,19} = 14\,853\,650 \text{ cycles}$$

(*b*) Gerber, Table 6–7

$$n_f = \frac{1}{2}\left(\frac{1295.8}{366.7}\right)^2\left(\frac{122.2}{235}\right)\left\{-1 + \sqrt{1 + \left[\frac{2(366.7)(235)}{1295.8(122.2)}\right]^2}\right\} = 1.55$$

Answer Thus, infinite life is predicted ($N \geq 10^6$ cycles).

EXAMPLE 6–12 A steel bar undergoes cyclic loading such that $\sigma_{max} = 60$ kpsi and $\sigma_{min} = -20$ kpsi. For the material, $S_{ut} = 80$ kpsi, $S_y = 65$ kpsi, a fully corrected endurance limit of $S_e = 40$ kpsi, and $f = 0.9$. Estimate the number of cycles to a fatigue failure using:

(*a*) Modified Goodman criterion.

(*b*) Gerber criterion.

Solution From the given stresses,

$$\sigma_a = \frac{60 - (-20)}{2} = 40 \text{ kpsi} \qquad \sigma_m = \frac{60 + (-20)}{2} = 20 \text{ kpsi}$$

From the material properties, Eqs. (6–14) to (6–16), p. 277, give

$$a = \frac{(f S_{ut})^2}{S_e} = \frac{[0.9(80)]^2}{40} = 129.6 \text{ kpsi}$$

$$b = -\frac{1}{3}\log\left(\frac{f S_{ut}}{S_e}\right) = -\frac{1}{3}\log\left[\frac{0.9(80)}{40}\right] = -0.0851$$

$$N = \left(\frac{S_f}{a}\right)^{1/b} = \left(\frac{S_f}{129.6}\right)^{-1/0.0851} \tag{1}$$

where S_f replaced σ_a in Eq. (6–16).

(*a*) The modified Goodman line is given by Eq. (6–46), p. 298, where the endurance limit S_e is used for infinite life. For finite life at $S_f > S_e$, replace S_e with S_f in Eq. (6–46) and rearrange giving

$$S_f = \frac{\sigma_a}{1 - \dfrac{\sigma_m}{S_{ut}}} = \frac{40}{1 - \dfrac{20}{80}} = 53.3 \text{ kpsi}$$

Substituting this into Eq. (1) yields

Answer

$$N = \left(\frac{53.3}{129.6}\right)^{-1/0.0851} \doteq 3.4(10^4) \text{ cycles}$$

(*b*) For Gerber, similar to part (*a*), from Eq. (6–47),

$$S_f = \frac{\sigma_a}{1 - \left(\dfrac{\sigma_m}{S_{ut}}\right)^2} = \frac{40}{1 - \left(\dfrac{20}{80}\right)^2} = 42.7 \text{ kpsi}$$

Again, from Eq. (1),

Answer

$$N = \left(\frac{42.7}{129.6}\right)^{-1/0.0851} \doteq 4.6(10^5) \text{ cycles}$$

Comparing the answers, we see a large difference in the results. Again, the modified Goodman criterion is conservative as compared to Gerber for which the moderate difference in S_f is then magnified by a logarithmic S, N relationship.

For many *brittle* materials, the first quadrant fatigue failure criteria follows a concave upward Smith-Dolan locus represented by

$$\frac{S_a}{S_e} = \frac{1 - S_m/S_{ut}}{1 + S_m/S_{ut}} \tag{6–50}$$

or as a design equation,

$$\frac{n\sigma_a}{S_e} = \frac{1 - n\sigma_m/S_{ut}}{1 + n\sigma_m/S_{ut}} \tag{6–51}$$

For a radial load line of slope r, we substitute S_a/r for S_m in Eq. (6–50) and solve for S_a, obtaining

$$S_a = \frac{rS_{ut} + S_e}{2}\left[-1 + \sqrt{1 + \frac{4rS_{ut}S_e}{(rS_{ut} + S_e)^2}}\right] \tag{6–52}$$

The fatigue diagram for a brittle material differs markedly from that of a ductile material because:

- Yielding is not involved since the material may not have a yield strength.
- Characteristically, the compressive ultimate strength exceeds the ultimate tensile strength severalfold.

- First-quadrant fatigue failure locus is concave-upward (Smith-Dolan), for example, and as flat as Goodman. Brittle materials are more sensitive to midrange stress, being lowered, but compressive midrange stresses are beneficial.
- Not enough work has been done on brittle fatigue to discover insightful generalities, so we stay in the first and a bit of the second quadrant.

The most likely domain of designer use is in the range from $-S_{ut} \leq \sigma_m \leq S_{ut}$. The locus in the first quadrant is Goodman, Smith-Dolan, or something in between. The portion of the second quadrant that is used is represented by a straight line between the points $-S_{ut}$, S_{ut} and 0, S_e, which has the equation

$$S_a = S_e + \left(\frac{S_e}{S_{ut}} - 1\right) S_m \qquad -S_{ut} \leq S_m \leq 0 \quad \text{(for cast iron)} \qquad (6\text{–}53)$$

Table A–24 gives properties of gray cast iron. The endurance limit stated is really $k_a k_b S'_e$ and only corrections k_c, k_d, k_e, and k_f need be made. The average k_c for axial and torsional loading is 0.9.

EXAMPLE 6–13 A grade 30 gray cast iron is subjected to a load F applied to a 25 by 10-mm cross-section link with a 6-mm-diameter hole drilled in the center as depicted in Fig. 6–32*a*. The surfaces are machined. In the neighborhood of the hole, what is the factor of safety guarding against failure under the following conditions:

(*a*) The load $F = 4500$ N tensile, steady.

(*b*) The load is 4500 N repeatedly applied.

(*c*) The load fluctuates between -4500 N and 1300 N without column action.

Use the Smith-Dolan fatigue locus.

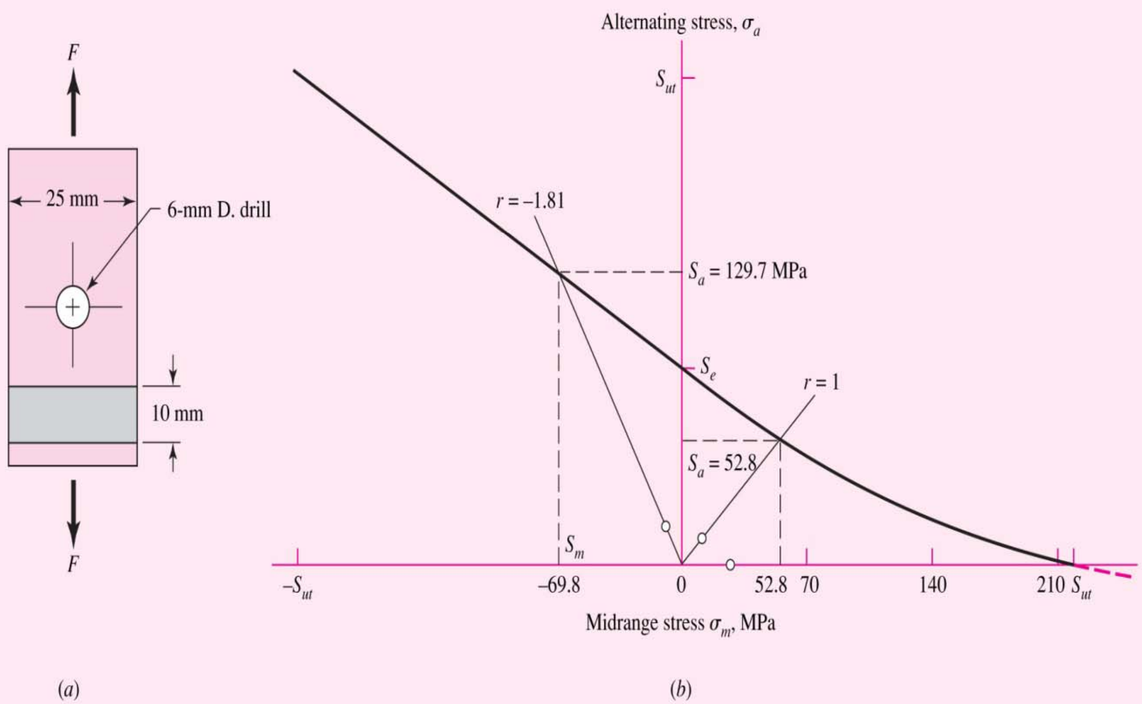

Figure 6–32

The grade 30 cast-iron part in axial fatigue with (*a*) its geometry displayed and (*b*) its designer's fatigue diagram for the circumstances of Ex. 6–13.

Solution Some preparatory work is needed. From Table A–24, $S_{ut} = 214$ MPa, $S_{uc} = 752$ MPa, $k_a k_b S'_e = 97$ MPa. Since k_c for axial loading is 0.9, then $S_e = (k_a k_b S'_e)k_c = 97(0.9) = 87.3$ MPa. From Table A–15–1, $A = t(w - d) = 0.01(0.025 - 0.006) = 190 \times 10^{-6}\ \mathrm{m}^2$, $d/w = 6/25 = 0.24$, and $K_t = 2.45$. The notch sensitivity for cast iron is 0.20 (see p. 296), so

$$K_f = 1 + q(K_t - 1) = 1 + 0.20(2.45 - 1) = 1.29$$

(*a*) $$\sigma_a = \frac{K_f F_a}{A} = \frac{1.29(0)}{A} = 0 \qquad \sigma_m = \frac{K_f F_m}{A} = \frac{1.29(4500)}{190 \times 10^{-6}} = 30.6\ \text{MPa}$$

and

Answer
$$n = \frac{S_{ut}}{\sigma_m} = \frac{214}{30.6} = 6.99$$

(*b*) $$F_a = F_m = \frac{F}{2} = \frac{4500}{2} = 2250\ \text{N}$$

$$\sigma_a = \sigma_m = \frac{K_f F_a}{A} = \frac{1.29(2250)}{190 \times 10^{-6}} = 15.3\ \text{MPa}$$

$$r = \frac{\sigma_a}{\sigma_m} = 1$$

From Eq. (6–52),

$$S_a = \frac{(1)31 + 12.6}{2}\left[-1 + \sqrt{1 + \frac{4(1)214(87.3)}{[(1)214 + 87.3]^2}}\,\right] = 52.8\ \text{MPa}$$

Answer

$$n = \frac{S_a}{\sigma_a} = \frac{52.8}{15.3} = 3.45$$

$$(c) \quad F_a = \frac{1}{2}|1300 - (-4500)| = 2900\text{ N} \quad \sigma_a = \frac{1.29(2900)}{190 \times 10^{-6}} = 19.7\text{ MPa}$$

$$F_m = \frac{1}{2}[1300 + (-4500)| = -1600\text{ N} \quad \sigma_m = \frac{1.29(-1600)}{190 \times 10^{-6}} = -10.9\text{ MPa}$$

$$r = \frac{\sigma_a}{\sigma_m} = \frac{19.7}{-10.9} = -1.81$$

From Eq. (6–53), $S_a = S_e + (S_e/S_{ut} - 1)S_m$ and $S_m = S_a/r$. It follows that

$$S_a = \frac{S_e}{1 - \dfrac{1}{r}\left(\dfrac{S_e}{S_{ut}} - 1\right)} = \frac{87.3}{1 - \dfrac{1}{-1.81}\left(\dfrac{87.3}{214} - 1\right)} = 129.7\text{ MPa}$$

Answer

$$n = \frac{S_a}{\sigma_a} = \frac{129.7}{19.7} = 6.58$$

Figure 6–32*b* shows the portion of the designer's fatigue diagram that was constructed.

Shaft Design for Stress : Stress Analysis

- Assuming a solid shaft with round cross section, appropriate geometry terms can be introduced for *c*, *I,* and *J* resulting in the fluctuating stresses due to bending and torsion as

$$\sigma_a = K_f \frac{32M_a}{\pi d^3} \qquad \sigma_m = K_f \frac{32M_m}{\pi d^3} \qquad \tau_a = K_{fs} \frac{16T_a}{\pi d^3} \qquad \tau_m = K_{fs} \frac{16T_m}{\pi d^3}$$

- Combining these stresses in accordance with the distortion energy failure theory, the von Mises stresses for rotating round, solid shafts, neglecting axial loads, are given by

$$\sigma_a' = (\sigma_a^2 + 3\tau_a^2)^{1/2} = \left[\left(\frac{32K_f M_a}{\pi d^3}\right)^2 + 3\left(\frac{16K_{fs}T_a}{\pi d^3}\right)^2\right]^{1/2} \qquad \sigma_m' = (\sigma_m^2 + 3\tau_m^2)^{1/2} = \left[\left(\frac{32K_f M_m}{\pi d^3}\right)^2 + 3\left(\frac{16K_{fs}T_m}{\pi d^3}\right)^2\right]^{1/2}$$

- These equivalent alternating and midrange stresses can be evaluated using an appropriate failure curve on the modified Goodman diagram as

$$\frac{1}{n} = \frac{\sigma_a'}{S_e} + \frac{\sigma_m'}{S_{ut}}$$

$$\frac{1}{n} = \frac{16}{\pi d^3}\left\{\frac{1}{S_e}\left[4(K_f M_a)^2 + 3(K_{fs}T_a)^2\right]^{1/2} + \frac{1}{S_{ut}}\left[4(K_f M_m)^2 + 3(K_{fs}T_m)^2\right]^{1/2}\right\}$$

- A von Mises maximum stress for static failure is calculated

$$\sigma_{\max}' = \left[(\sigma_m + \sigma_a)^2 + 3(\tau_m + \tau_a)^2\right]^{1/2}$$

$$= \left[\left(\frac{32K_f(M_m + M_a)}{\pi d^3}\right)^2 + 3\left(\frac{16K_{fs}(T_m + T_a)}{\pi d^3}\right)^2\right]^{1/2}$$

$$d = \left(\frac{16n}{\pi} \left\{ \frac{1}{S_e} \left[4(K_f M_a)^2 + 3(K_{fs} T_a)^2 \right]^{1/2} + \frac{1}{S_{ut}} \left[4(K_f M_m)^2 + 3(K_{fs} T_m)^2 \right]^{1/2} \right\} \right)^{1/3}$$

DE-Goodman

$$\frac{1}{n} = \frac{16}{\pi d^3} \left\{ \frac{1}{S_e} \left[4(K_f M_a)^2 + 3(K_{fs} T_a)^2 \right]^{1/2} + \frac{1}{S_{ut}} \left[4(K_f M_m)^2 + 3(K_{fs} T_m)^2 \right]^{1/2} \right\} \qquad (7\text{–}7)$$

$$d = \left(\frac{16n}{\pi} \left\{ \frac{1}{S_e} \left[4(K_f M_a)^2 + 3(K_{fs} T_a)^2 \right]^{1/2} + \frac{1}{S_{ut}} \left[4(K_f M_m)^2 + 3(K_{fs} T_m)^2 \right]^{1/2} \right\} \right)^{1/3} \qquad (7\text{–}8)$$

DE-Gerber

$$\frac{1}{n} = \frac{8A}{\pi d^3 S_e}\left\{1 + \left[1 + \left(\frac{2BS_e}{AS_{ut}}\right)^2\right]^{1/2}\right\} \tag{7–9}$$

$$d = \left(\frac{8nA}{\pi S_e}\left\{1 + \left[1 + \left(\frac{2BS_e}{AS_{ut}}\right)^2\right]^{1/2}\right\}\right)^{1/3} \tag{7–10}$$

where

$$A = \sqrt{4(K_f M_a)^2 + 3(K_{fs} T_a)^2}$$

$$B = \sqrt{4(K_f M_m)^2 + 3(K_{fs} T_m)^2}$$

DE-ASME Elliptic

$$\frac{1}{n} = \frac{16}{\pi d^3}\left[4\left(\frac{K_f M_a}{S_e}\right)^2 + 3\left(\frac{K_{fs} T_a}{S_e}\right)^2 + 4\left(\frac{K_f M_m}{S_y}\right)^2 + 3\left(\frac{K_{fs} T_m}{S_y}\right)^2\right]^{1/2} \tag{7–11}$$

$$d = \left\{\frac{16n}{\pi}\left[4\left(\frac{K_f M_a}{S_e}\right)^2 + 3\left(\frac{K_{fs} T_a}{S_e}\right)^2 + 4\left(\frac{K_f M_m}{S_y}\right)^2 + 3\left(\frac{K_{fs} T_m}{S_y}\right)^2\right]^{1/2}\right\}^{1/3} \tag{7–12}$$

DE-Soderberg

$$\frac{1}{n} = \frac{16}{\pi d^3} \left\{ \frac{1}{S_e} \left[4(K_f M_a)^2 + 3(K_{fs} T_a)^2 \right]^{1/2} + \frac{1}{S_{yt}} \left[4(K_f M_m)^2 + 3(K_{fs} T_m)^2 \right]^{1/2} \right\} \tag{7–13}$$

$$d = \left(\frac{16n}{\pi} \left\{ \frac{1}{S_e} \left[4(K_f M_a)^2 + 3(K_{fs} T_a)^2 \right]^{1/2} + \frac{1}{S_{yt}} \left[4(K_f M_m)^2 + 3(K_{fs} T_m)^2 \right]^{1/2} \right\} \right)^{1/3} \tag{7–14}$$

Fig. 6–27. The Gerber and modified Goodman criteria do not guard against yielding, requiring a separate check for yielding. A von Mises maximum stress is calculated for this purpose.

$$\sigma'_{max} = \left[(\sigma_m + \sigma_a)^2 + 3(\tau_m + \tau_a)^2\right]^{1/2}$$

$$= \left[\left(\frac{32K_f(M_m + M_a)}{\pi d^3}\right)^2 + 3\left(\frac{16K_{fs}(T_m + T_a)}{\pi d^3}\right)^2\right]^{1/2} \tag{7–15}$$

To check for yielding, this von Mises maximum stress is compared to the yield strength, as usual.

$$n_y = \frac{S_y}{\sigma'_{max}} \tag{7–16}$$

For a quick, conservative check, an estimate for σ'_{max} can be obtained by simply adding σ'_a and σ'_m. $(\sigma'_a + \sigma'_m)$ will always be greater than or equal to σ'_{max}, and will therefore be conservative.

Shaft Design for Stress : Stress Concentration

- Stress concentrations for shoulders and keyways are dependent on size specifications that are not known the first time through the process.
- These stress concentrations will be fine-tuned in successive iterations, once the details are known.
- In cases where the shoulder at the bearing is found to be critical, the designer should plan to select a bearing with generous fillet radius, or consider providing for a larger fillet radius on the shaft by relieving it into the base of the shoulder.
- A keyway will produce a stress concentration near a critical point where the load-transmitting component is located.
- Some typical stress concentration facto iteration in the design of a shaft.

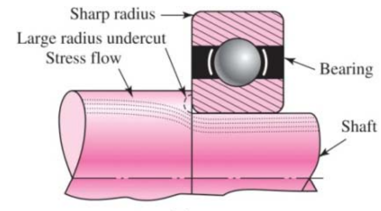

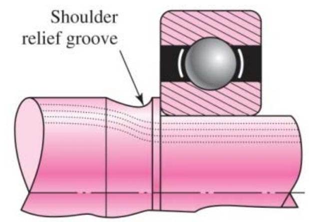

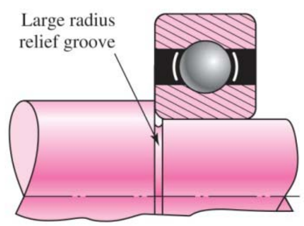

	Bending	Torsional	Axial
Shoulder fillet—sharp (r/d = 0.02)	2.7	2.2	3.0
Shoulder fillet—well rounded (r/d = 0.1)	1.7	1.5	1.9
End-mill keyseat (r/d = 0.02)	2.14	3.0	—
Sled runner keyseat	1.7	—	—
Retaining ring groove	5.0	3.0	5.0

Missing values in the table are not readily available.

EXAMPLE 7–1 At a machined shaft shoulder the small diameter d is 28 mm, the large diameter D is 42 mm, and the fillet radius is 2.8 mm. The bending moment is 142.4 N·m and the steady torsion moment is 124.3 N·m. The heat-treated steel shaft has an ultimate strength of $S_{ut} = 735$ MPa and a yield strength of $S_y = 574$ MPa. The reliability goal is 0.99.

(a) Determine the fatigue factor of safety of the design using each of the fatigue failure criteria described in this section.

(b) Determine the yielding factor of safety.

Solution (*a*) $D/d = 42/28 = 1.50$, $r/d = 2.8/28 = 0.10$, $K_t = 1.68$ (Fig. A–15–9), $K_{ts} = 1.42$ (Fig. A–15–8), $q = 0.85$ (Fig. 6–20), $q_{\text{shear}} = 0.92$ (Fig. 6–21).

From Eq. (6–32),

$$K_f = 1 + 0.85(1.68 - 1) = 1.58$$

$$K_{fs} = 1 + 0.92(1.42 - 1) = 1.39$$

Eq. (6–8): $$S'_e = 0.5(735) = 367.5 \text{ MPa}$$

Eq. (6–19): $$k_a = 4.51(735)^{-0.265} = 0.787$$

Eq. (6–20): $$k_b = \left(\frac{28}{7.62}\right)^{-0.107} = 0.870$$

$$k_c = k_d = k_f = 1$$

Table 6–6: $$k_e = 0.814$$

$$S_e = 0.787(0.870)0.814(367.5) = 205 \text{ MPa}$$

For a rotating shaft, the constant bending moment will create a completely reversed bending stress.

$$M_a = 142.4 \text{ N·m} \qquad T_m = 124.3 \text{ N·m} \qquad M_m = T_a = 0$$

Applying Eq. (7–7) for the DE-Goodman criteria gives

$$\frac{1}{n}=\frac{16}{\pi(0.028)^3}\left\{\frac{\left[4(1.58\cdot 142.4)^2\right]^{1/2}}{205\times 10^6}+\frac{\left[3(1.39\cdot 124.3)^2\right]^{1/2}}{735\times 10^6}\right\}=0.615$$

Answer $$n=1.62 \qquad \text{DE-Goodman}$$

Similarly, applying Eqs. (7–9), (7–11), and (7–13) for the other failure criteria,

Answer $$n=1.87 \qquad \text{DE-Gerber}$$

Answer $$n=1.88 \qquad \text{DE-ASME Elliptic}$$

Answer $$n=1.56 \qquad \text{DE-Soderberg}$$

For comparison, consider an equivalent approach of calculating the stresses and applying the fatigue failure criteria directly. From Eqs. (7–5) and (7–6),

$$\sigma'_a=\left[\left(\frac{32\cdot 1.58\cdot 142.4}{\pi(0.028)^3}\right)^2\right]^{1/2}=104.4\ \text{MPa}$$

$$\sigma'_m=\left[3\left(\frac{16\cdot 1.39\cdot 124.3}{\pi(0.028)^3}\right)^2\right]^{1/2}=69.4\ \text{MPa}$$

Taking, for example, the Goodman failure critera, application of Eq. (6–46) gives

Taking, for example, the Goodman failure critera, application of Eq. (6–46) gives

$$\frac{1}{n} = \frac{\sigma'_a}{S_e} + \frac{\sigma'_m}{S_{ut}} = \frac{104.4}{205} + \frac{69.4}{735} = 0.604$$

$$n = 1.62$$

which is identical with the previous result. The same process could be used for the other failure criteria.

(*b*) For the yielding factor of safety, determine an equivalent von Mises maximum stress using Eq. (7–15).

$$\sigma'_{\max} = \left[\left(\frac{32(1.58)\,(142.4)}{\pi\,(0.028)^3}\right)^2 + 3\left(\frac{16(1.39)\,(124.3)}{\pi\,(0.028)^3}\right)^2\right]^{1/2} = 125.4\ \text{MPa}$$

Answer

$$n_y = \frac{S_y}{\sigma'_{\max}} = \frac{574}{125.4} = 4.58$$

For comparison, a quick and very conservative check on yielding can be obtained by replacing $\sigma'_{\max}$ with $\sigma'_a + \sigma'_m$. This just saves the extra time of calculating $\sigma'_{\max}$ if σ'_a and σ'_m have already been determined. For this example,

$$n_y = \frac{S_y}{\sigma'_a + \sigma'_m} = \frac{574}{104.4 + 69.4} = 3.3$$

which is quite conservative compared with $n_y = 4.58$.

EXAMPLE 7–2

This example problem is part of a larger case study. See Chap. 18 for the full context.

A double reduction gearbox design has developed to the point that the general layout and axial dimensions of the countershaft carrying two spur gears has been proposed, as shown in Fig. 7–10. The gears and bearings are located and supported by shoulders, and held in place by retaining rings. The gears transmit torque through keys. Gears have been specified as shown, allowing the tangential and radial forces transmitted through the gears to the shaft to be determined as follows.

$$W_{23}^{t} = 2400\ \text{N} \qquad W_{54}^{t} = -10\,800\ \text{N}$$

$$W_{23}^{r} = -870\ \text{N} \qquad W_{54}^{r} = -3900\ \text{N}$$

where the superscripts *t* and *r* represent tangential and radial directions, respectively; and, the subscripts 23 and 54 represent the forces exerted *by* gears 2 and 5 (not shown) *on* gears 3 and 4, respectively.

Proceed with the next phase of the design, in which a suitable material is selected, and appropriate diameters for each section of the shaft are estimated, based on providing sufficient fatigue and static stress capacity for infinite life of the shaft, with minimum safety factors of 1.5.

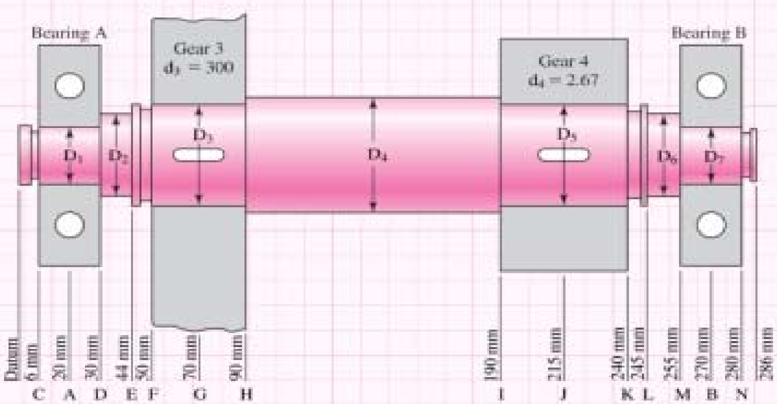

Figure 7–10

Shaft layout for Ex. 7–2. Dimensions in millimeters.

Solution

Perform free body diagram analysis to get reaction forces at the bearings.

$R_{Az} = 422$ N

$R_{Ay} = 1439$ N

$R_{Bz} = 8822$ N

$R_{By} = 3331$ N

From ΣM_x, find the torque in the shaft between the gears, $T = W^t_{23}(d_3/2) = 2400\ (0.3/2) = 360$ N·m

Generate shear-moment diagrams for two planes.

Combine orthogonal planes as vectors to get total moments, e.g. at J, $\sqrt{485^2 + 183^2} = 518$ N·m.

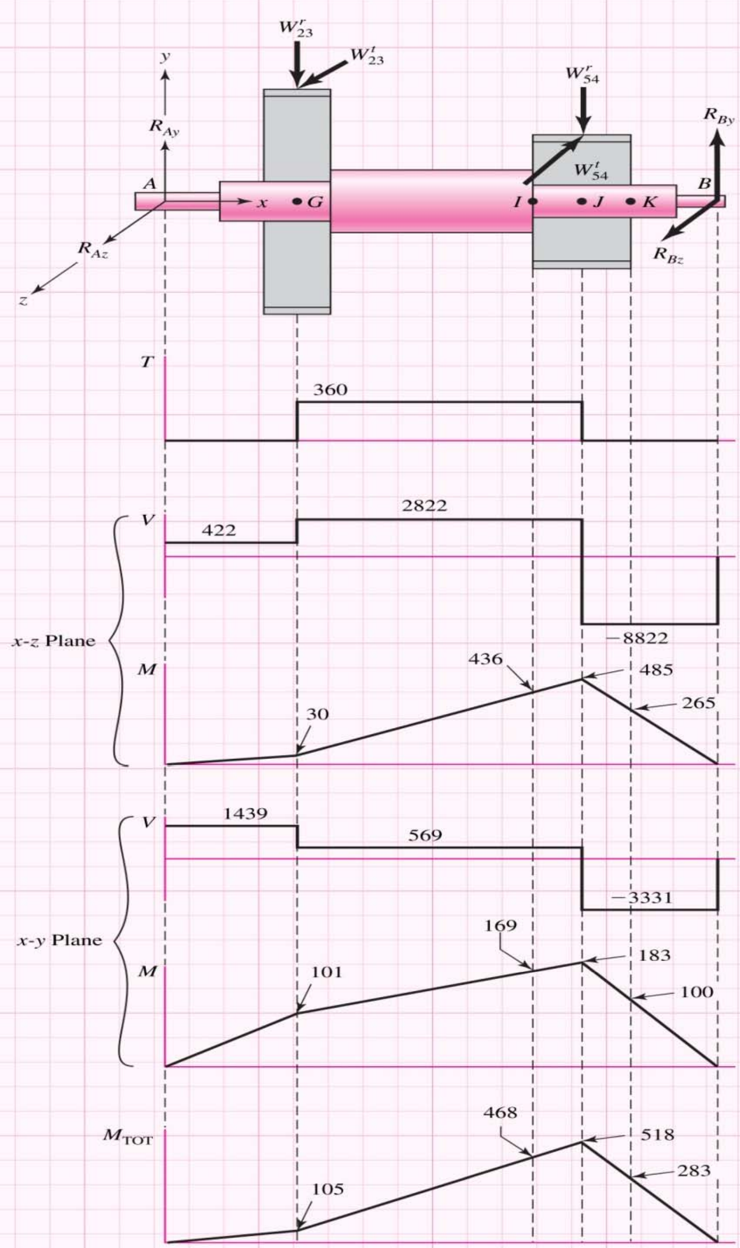

Start with Point I, where the bending moment is high, there is a stress concentration at the shoulder, and the torque is present.

$$\text{At } I,\ M_a = 468 \text{ N·m},\quad T_m = 360 \text{ N·m},\quad M_m = T_a = 0$$

Assume generous fillet radius for gear at I.

From Table 7–1, estimate $K_t = 1.7$, $K_{ts} = 1.5$. For quick, conservative first pass, assume $K_f = K_t$, $K_{fs} = K_{ts}$.

Choose inexpensive steel, 1020 CD, with $S_{ut} = 469$ MPa. For S_e,

Eq. (6–19) $\quad k_a = aS_{ut}^b = 4.51\,(469)^{-0.265} = 0.883$

Guess $k_b = 0.9$. Check later when d is known.

$$k_c = k_d = k_e = 1$$

Eq. (6–18) $\quad S_e = (0.883)(0.9)(0.5)(469) = 186$ MPa.

For first estimate of the small diameter at the shoulder at point I, use the DE-Goodman criterion of Eq. (7–8). This criterion is good for the initial design, since it is simple and conservative. With $M_m = T_a = 0$, Eq. (7–8) reduces to

$$d = \left\{ \frac{16n}{\pi} \left(\frac{2\,(K_f M_a)}{S_e} + \frac{\left[3\,(K_{fs} T_m)^2\right]^{1/2}}{S_{ut}} \right) \right\}^{1/3}$$

$$d = \left\{ \frac{16(1.5)}{\pi} \left(\frac{2\,(1.7)\,(468)}{186 \times 10^6} + \frac{\{3\,[(1.5)\,(360)]^2\}^{1/2}}{469 \times 10^6} \right) \right\}^{1/3}$$

$$d = 0.0432 \text{ m} = 43.2 \text{ mm}$$

All estimates have probably been conservative, so select the next standard size below 43.2 m. and check, $d = 42$ mm.

A typical D/d ratio for support at a shoulder is $D/d = 1.2$, thus, $D = 1.2 \times 42 = 50.4$ mm. Use D = 50 mm. A nominal 50-mm cold-drawn shaft diameter can be used. Check if estimates were acceptable.

$$D/d = 50/42 = 1.19$$

Assume fillet radius $r = d/10 \cong 4$ mm $\qquad r/d = 0.1$

$$K_t = 1.6 \text{ (Fig. A–15–9)}, \ q = 0.82 \text{ (Fig. 6–20)}$$

Eq. (6–32) $\quad K_f = 1 + 0.82(1.6 - 1) = 1.49$

$$K_{ts} = 1.35 \quad \text{(Fig. A–15–8)}, \ q_s = 0.95 \text{ (Fig. 6–21)}$$

$$K_{fs} = 1 + 0.95(1.35 - 1) = 1.33$$

$$k_a = 0.883 \text{ (no change)}$$

Eq. (6–20) $\quad k_b = \left(\dfrac{42}{7.62}\right)^{-0.107} = 0.833$

$$S_e = (0.883)(0.833)(0.5)(469) = 172 \text{ MPa}$$

Eq. (7–5) $\quad \sigma'_a = \dfrac{32K_f M_a}{\pi d^3} = \dfrac{32(1.49)(468)}{\pi(0.042)^3} = 96$ MPa

Eq. (7–6) $\quad \tau'_m = \left[3\left(\dfrac{16K_{fs}T_m}{\pi d^3}\right)^2\right]^{1/2} = \dfrac{\sqrt{3}(16)(1.33)(360)}{\pi(0.042)^3} = 57$ MPa

Using Goodman criterion

$$\frac{1}{n_f} = \frac{\sigma'_a}{S_e} + \frac{\sigma'_m}{S_{ut}} = \frac{96}{172} + \frac{57}{469} = 0.68$$

$$n_f = 1.55$$

Note that we could have used Eq. (7–7) directly.
Check yielding.

$$n_y = \frac{S_y}{\sigma'_{\max}} > \frac{S_y}{\sigma'_a + \sigma'_m} = \frac{393}{96 + 57} = 2.57$$

Also check this diameter at the end of the keyway, just to the right of point I, and at the groove at point K. From moment diagram, estimate M at end of keyway to be $M = 443\ \text{N}\cdot\text{m}$.

Assume the radius at the bottom of the keyway will be the standard $r/d = 0.02$, $r = 0.02\,d = 0.02\,(42) = 0.84$ mm

$$K_t = 2.14 \text{ (Fig. A–15–18)}, \; q = 0.65 \text{ (Fig. 6–20)}$$

$$K_f = 1 + 0.65(2.14 - 1) = 1.74$$

$$K_{ts} = 3.0 \text{ (Fig. A–15–19)}, \; q_s = 0.9 \text{ (Fig. 6–21)}$$

$$K_{fs} = 1 + 0.9(3 - 1) = 2.8$$

$$\sigma'_a = \frac{32 K_f M_a}{\pi d^3} = \frac{32(1.74)(443)}{\pi (0.042)^3} = 106 \text{ MPa}$$

$$\sigma'_m = \sqrt{3}(16)\frac{K_{fs} T_m}{\pi d^3} = \frac{\sqrt{3}(16)(2.8)(443)}{\pi (0.042)^3} = 148 \text{ MPa}$$

$$\frac{1}{n_f} = \frac{\sigma'_a}{S_e} + \frac{\sigma'_m}{S_{ut}} = \frac{106}{172} + \frac{148}{469} = 0.93$$

$$n_f = 1.08$$

The keyway turns out to be more critical than the shoulder. We can either increase the diameter, or use a higher strength material. Unless the deflection analysis shows a need for larger diameters, let us choose to increase the strength. We started with a very low strength, and can afford to increase it some to avoid larger sizes. Try 1050 CD, with $S_{ut} = 690$ MPa.

Recalculate factors affected by S_{ut}, i.e. $k_a \rightarrow S_e$; $q \rightarrow K_f \rightarrow \sigma'_a$

$$k_a = 4.51(690)^{-0.265} = 0.797, \quad S_e = 0.797(0.833)(0.5)(690) = 229 \text{ MPa}$$

$$q = 0.72, \; K_f = 1 + 0.72(2.14 - 1) = 1.82$$

$$\sigma'_a = \frac{32(1.82)(443)}{\pi (0.042)^3} = 110.8 \text{ MPa}$$

$$\frac{1}{n_f} = \frac{110.8}{229} + \frac{148}{690} = 0.7$$

$$n_f = 1.43$$

Since the Goodman criterion is conservative, we will accept this as close enough to the requested 1.5.

Check at the groove at K, since K_t for flat-bottomed grooves are often very high. From the torque diagram, note that no torque is present at the groove. From the moment diagram, $M_a = 283\ \text{N}\cdot\text{m}$, $M_m = T_a = T_m = 0$. To quickly check if this location is potentially critical just use $K_f = K_t = 5.0$ as an estimate, from Table 7–1.

$$\sigma_a = \frac{32 K_f M_a}{\pi d^3} = \frac{32(5)(283)}{\pi (0.042)^3} = 194.5 \text{ MPa}$$

$$n_f = \frac{S_e}{\sigma_a} = \frac{229}{194.5} = 1.18$$

This is low. We will look up data for a specific retaining ring to obtain K_f more accurately. With a quick on-line search of a retaining ring specification using the website www.globalspec.com, appropriate groove specifications for a retaining ring for a shaft diameter of 42 mm are obtained as follows: width, $a = 1.73$ mm; depth, $t = 1.22$ mm; and corner radius at bottom of groove, $r = 0.25$ mm.
From Fig. A–15–16, with $r/t = 0.25/1.22 = 0.205$, and $a/t = 1.73/1.22 = 1.42$

$$K_t = 4.3,\ q = 0.65\ \text{(Fig. 6–20)}$$

$$K_f = 1 + 0.65(4.3 - 1) = 3.15$$

$$\sigma_a = \frac{32K_f M_a}{\pi d^3} = \frac{32(3.15)(283)}{\pi(0.042)^3} = 122.6\ \text{MPa}$$

$$n_f = \frac{S_e}{\sigma_a} = \frac{229}{122.6} = 1.87$$

Quickly check if point M might be critical. Only bending is present, and the moment is small, but the diameter is small and the stress concentration is high for a sharp fillet required for a bearing. From the moment diagram,
$M_a = 113\ \text{N}\cdot\text{m}$, and $M_m = T_m = T_a = 0$.

Estimate $K_t = 2.7$ from Table 7–1, $d = 25$ mm, and fillet radius r to fit a typical bearing.

$$r/d = 0.02,\ r = 0.02(25) = 0.5$$

$$q = 0.7\ \text{(Fig. 6–20)}$$

$$K_f = 1 + (0.7)(2.7 - 1) = 2.19$$

$$\sigma_a = \frac{32K_f M_a}{\pi d^3} = \frac{32(2.19)(113)}{\pi(0.025)^3} = 161\ \text{MPa}$$

$$n_f = \frac{S_e}{\sigma_a} = \frac{229}{161} = 1.42$$

Should be OK. Close enough to recheck after bearing is selected.

With the diameters specified for the critical locations, fill in trial values for the rest of the diameters, taking into account typical shoulder heights for bearing and gear support.

$$D_1 = D_7 = 25\ \text{mm}$$

$$D_2 = D_6 = 35\ \text{mm}$$

$$D_3 = D_5 = 42\ \text{mm}$$

$$D_4 = 50\ \text{mm}$$

The bending moments are much less on the left end of shaft, so D_1, D_2, and D_3 could be smaller. However, unless weight is an issue, there is little advantage to requiring more material removal. Also, the extra rigidity may be needed to keep deflections small.